

# Set-based state estimation of nonlinear discrete-time systems using constrained zonotopes and polyhedral relaxations<sup>\*</sup>

Brenner S. Rego<sup>a,\*</sup>, Guilherme V. Raffo<sup>b</sup>, Marco H. Terra<sup>a</sup>, Joseph K. Scott<sup>c</sup>

<sup>a</sup>Department of Electrical and Computer Engineering, University of São Paulo, São Carlos, SP 13566-590, Brazil

<sup>b</sup>Department of Electronics Engineering, Federal University of Minas Gerais, Belo Horizonte, MG 31270-901, Brazil

<sup>c</sup>Department of Chemical and Biomolecular Engineering, Georgia Institute of Technology, 311 Ferst Dr., Atlanta, 30318, GA, USA

## Abstract

This paper presents a new algorithm for set-based state estimation of nonlinear discrete-time systems with bounded uncertainties. The novel method builds upon essential properties and computational advantages of constrained zonotopes (CZs) and polyhedral relaxations of factorable representations of nonlinear functions to propagate CZs through nonlinear functions, which is usually done using conservative linearization in the literature. The new method also refines the propagated enclosure using nonlinear measurements. To achieve this, a lifted polyhedral relaxation is computed for the composite nonlinear function of the system dynamics and measurement equations, in addition to incorporating the measured output through equality constraints. Polyhedral relaxations of trigonometric functions are enabled for the first time, allowing to address a broader class of nonlinear systems than our previous works. Additionally, an approach to obtain an equivalent enclosure with fewer generators and constraints is developed. Thanks to the advantages of the polyhedral enclosures based on factorable representations, the new state estimation method provides better approximations than those resulting from linearization procedures. This led to significant improvements in the computation of convex sets enclosing the system states consistent with measured outputs. Numerical examples highlight the advantages of the novel algorithm in comparison to existing CZ methods based on the Mean Value Theorem and DC programming principles.

**Keywords:** Nonlinear observers, Constrained zonotopes, Convex polytopes, Reachability analysis

## 1. Introduction

This paper develops a new method for set-based state estimation for nonlinear discrete-time systems with bounded uncertainties. Set-based methods are able to generate guaranteed enclosures of the system trajectories. Unlike stochastic strategies, such as the Kalman filter (Simon, 2010), these methods do not require knowledge of the stochastic properties of the uncertainties. In these lines, reachability analysis and set-based state estimation of dynamical systems are important topics in the recent literature (Yang & Scott, 2020; Althoff et al., 2021; Rego et al., 2022; Mu & Scott, 2024). The former consists of obtaining guaranteed system state enclosures for an uncertain initial set and bounded disturbances. At the same time, the latter also refines the guaranteed enclosures using the system outputs. In the general case, both the system dynamics and measurements are nonlinear, which result in an open problem consisting of significant challenges to obtain tight enclosures while maintaining reasonable computational complexity.

Methods for set-based state estimation of nonlinear systems have been built upon many different set representations, such

as ellipsoids (Wang et al., 2022), convex polytopes (Shamma & Tu, 1997), interval arithmetic (Jaulin, 2016), zonotopes (Alamo et al., 2005; Combastel, 2005), and generalizations of zonotopes, such as constrained zonotopes (CZs) (Rego et al., 2021), constrained polynomial zonotopes (Kochdumper & Althoff, 2023), hybrid zonotopes (Siefert et al., 2024), and constrained convex generators (Silvestre, 2022). This work focuses on methods based on zonotopes and constrained zonotopes, thanks to their computational advantages for some important set operations, and to the availability of polynomial-time complexity reduction algorithms (Scott et al., 2016; Yang & Scott, 2018b; Raghuraman & Koeln, 2022).

The core of set-based state estimation consists in propagating sets through nonlinear functions, and refining the resulting enclosure using measured outputs. Additionally, the computation of this enclosure often results in a complexity increase of the set representation at each time step, which can be a prohibitive factor for certain approximation methods if not addressed carefully. Most of the set-based state estimation methods based on zonotopes and CZs in the literature rely on linear approximation of the nonlinear functions, with often conservative bounds on the linearization error. The enclosures on the linearization error are generally obtained by using either the Mean Value Theorem or the Taylor's Theorem (Alamo et al., 2005; Combastel, 2005; Rego et al., 2021). For small uncertainties, these linear approximations may result in good enclosures. However, since the function is linearized with error bounds valid on the en-

<sup>\*</sup>This work was partially supported by the Brazilian agencies CNPq, under grants 465755/2014-3 (INCT project), and 315695/2020-0; FAPESP, under the grants 2014/50851-0, 2022/05052-8 and 2023/06896-8; CAPES, under the grants 001 and 88887.136349/2017-00; and FAPEMIG, under grant APQ-03090-17.

\*Corresponding author, [brennersr7@usp.br](mailto:brennersr7@usp.br)

tire state enclosure, severe conservatism is observed for larger sets. This occurs even if the previous bounds correspond to the exact state set consistent with the measurements, resulting in impractical enclosures of the system states. As an alternative to the Mean Value Theorem and the Taylor’s Theorem, DC programming principles can be used to obtain improved bounds on the linearization error (Alamo et al., 2008; de Paula et al., 2024). However, these algorithms have exponential complexity in the system dimension, and the resulting enclosures may not be accurate for some functional forms (Tottoli et al., 2023). Additional zonotope methods based on the Koopman operator can be found in the literature (Pan & Liu, 2023), which do not require the computation of enclosures for the linearization error. Instead, these methods rely on building variable transformations to a lifted space in which the dynamics and measurement equations are linear. Nevertheless, for general functional forms, state estimation methods based on such an operator may require infinite-dimensional representations for reliable approximations of the nonlinear functions composing the system dynamics and measurements.

In this work, we develop a novel methodology for state estimation of nonlinear discrete-time systems with bounded uncertainties using constrained zonotopes and polyhedral relaxations, denoted as CZPR. The proposed algorithm allows for the propagation of CZs through nonlinear dynamics, in addition to refinement of the enclosures using nonlinear measurement equations, without requiring linearization or the computation of linearization errors. The new propagation algorithm builds upon a common methodology used in the global optimization literature for the computation of linear programming relaxations of nonlinear optimization problems (Tawarmalani & Sahinidis, 2002, 2005). In this method, the nonlinear function is decomposed into a *factorable representation*, consisting of an equivalent sequence of elementary operations providing the same nonlinear mapping. Enclosing each one of these operations by a convex polytope allows for the generation of a polyhedral relaxation in a lifted space, which can provide less conservative boundaries than linearization methods. In this work, this polyhedral enclosure is generated using the factorable representation of the composite nonlinear function of the system dynamics and measurement equations, in addition to incorporating the measured output through equality constraints. Properties of CZs are then employed in the projection of the enclosure into the system dynamics’ image space. Constrained zonotopes extend zonotopes by adding equality constraints (Scott et al., 2016), allowing to describe arbitrary convex polytopes, whereas keeping most of the computational benefits of zonotopes in comparison to pure polytope computations (Kühn, 1998). This results in a new recursive state estimation method with linear complexity increase of the CZs at each time step, while providing a significant improvement in comparison to other CZ methods from the literature based on the Mean Value Theorem (Rego et al., 2021) and DC programming principles (de Paula et al., 2024). The complexity increase can be addressed by using polynomial-time complexity reduction algorithms for CZs (Scott et al., 2016).

This paper extends and improves on our previous results ob-

tained in Rego et al. (2024) as follows:

- The CZ propagation method is extended to incorporate measured outputs, effectively allowing for state estimation of nonlinear discrete-time systems,
- Polyhedral relaxations of trigonometric functions are developed for the first time, expanding the library of elementary operations allowed for factorable representation of nonlinear functions to which the new method can be applied,
- An equivalent CZ enclosure with less generators and constraints is proposed, leading to less computational cost without introducing conservatism,
- It presents a more sophisticated and clear formulation of the concepts and methods involved, and
- We evaluate the proposed method in challenging numerical examples for state estimation that require the improvements above.

The manuscript is organized as follows. The state estimation problem is stated in Section 2, along with necessary mathematical background for the paper. Section 3 describes a method to obtain a lifted halfspace enclosure of the image of a nonlinear function over an interval. Section 4 builds upon the lifted enclosure to enable the propagation of CZs through nonlinear functions, in addition to the refinement of such enclosures using nonlinear measurements, allowing the recursive use of such enclosures for set-based state estimation. Numerical examples are presented in Section 5. Section 6 concludes the paper.

## 2. Preliminaries and problem formulation

### 2.1. Interval analysis

Let  $\mathbb{IR}^n$  denote the set of all non-empty compact intervals in  $\mathbb{R}^n$ . For endpoints  $\mathbf{x}^L, \mathbf{x}^U \in \mathbb{R}^n$  with  $\mathbf{x}^L \leq \mathbf{x}^U$ , an *interval*  $X \in \mathbb{IR}^n$  is defined as  $X \triangleq \{\mathbf{x} \in \mathbb{R}^n : \mathbf{x}^L \leq \mathbf{x} \leq \mathbf{x}^U\} \triangleq [\mathbf{x}^L, \mathbf{x}^U]$ . In addition,  $\text{mid}(X) \triangleq \frac{1}{2}(\mathbf{x}^U + \mathbf{x}^L) \triangleq \mathbf{x}^M$ ,  $\text{rad}(X) \triangleq \frac{1}{2}(\mathbf{x}^U - \mathbf{x}^L) \triangleq \mathbf{x}^R$ , and  $B_\infty^n \triangleq [-\mathbf{1}_{n \times 1}, \mathbf{1}_{n \times 1}]$ .

Let  $X \triangleq [x^L, x^U] \in \mathbb{IR}$  and  $W \triangleq [w^L, w^U] \in \mathbb{IR}$ . Then, for any of the four basic arithmetic operations  $\odot \in \{+, -, \times, /\}$ , we define  $X \odot W \triangleq \{x \odot w : x \in X, w \in W\}$  (division is undefined if  $0 \in W$ ). Moreover, accurate interval bounds for the image of elementary nonlinear functions  $h : X \subset \mathbb{R} \rightarrow \mathbb{R}$  over an interval domain  $X \in \mathbb{IR}$ , such as the power, exponential, logarithm, and trigonometric functions, are easily obtainable through interval arithmetic. Simple formulas for computing all of these operations in terms of the input endpoints can be found in Moore et al. (2009).

### 2.2. Factorable functions

In this paper, we consider nonlinear functions that are *factorable* as defined below. This definition refers to a library  $\mathcal{L}$  of *intrinsic univariate functions*, which typically contains the functions in a standard math library in any programming language, such as  $x^a$ ,  $e^x$ ,  $\ln(x)$ ,  $\sin x$ , etc.

**Definition 1.** A function  $\varphi : D \subseteq \mathbb{R}^{n_s} \rightarrow \mathbb{R}^{n_\varphi}$  is said to be *factorable* if it can be expressed in terms of a finite sequence of *factors*  $\zeta_j : D \rightarrow \mathbb{R}$  with  $j \in \{1, \dots, n_z\}$  such that:

1. For each  $j \leq n_s$ ,  $\zeta_j(\mathbf{s}) = s_j$ ,  $\forall \mathbf{s} \in D$ ;
2. For each  $j > n_s$ , either
  - (a)  $\zeta_j(\mathbf{s}) \triangleq \zeta_a(\mathbf{s}) \odot \zeta_b(\mathbf{s})$ ,  $\forall \mathbf{s} \in D$ , where  $a, b < j$  and  $\odot \in \{+, -, \times, /$ , or
  - (b)  $\zeta_j(\mathbf{s}) \triangleq \beta_j(\zeta_a(\mathbf{s}))$ ,  $\forall \mathbf{s} \in D$ , where  $a < j$  and  $\beta_j$  is an intrinsic univariate function in  $\mathcal{L}$ ;
3.  $\varphi(\mathbf{s}) = \mathbf{E}_\varphi \boldsymbol{\zeta}(\mathbf{s})$ , where  $\boldsymbol{\zeta} = (\zeta_1, \dots, \zeta_{n_z})$  and  $\mathbf{E}_\varphi \in \mathbb{R}^{n_\varphi \times n_z}$  is a matrix of zeros except for a single 1 in each of its rows (i.e., each output is an element of  $\boldsymbol{\zeta}$ ).

For illustration purposes, let

$$\varphi(\mathbf{s}) \triangleq \frac{s_1}{s_2 s_3 \sqrt[3]{\frac{(s_2 + s_3)}{3}}}.$$

This function can be factorized as  $\zeta_1(\mathbf{s}) \triangleq s_1$ ,  $\zeta_2(\mathbf{s}) \triangleq s_2$ ,  $\zeta_3(\mathbf{s}) \triangleq s_3$ ,

$$\begin{aligned} \zeta_4(\mathbf{s}) &\triangleq \zeta_2(\mathbf{s})\zeta_3(\mathbf{s}), & \zeta_7(\mathbf{s}) &\triangleq \sqrt[3]{\zeta_6(\mathbf{s})}, \\ \zeta_5(\mathbf{s}) &\triangleq \zeta_2(\mathbf{s}) + \zeta_3(\mathbf{s}), & \zeta_8(\mathbf{s}) &\triangleq \zeta_4(\mathbf{s})\zeta_7(\mathbf{s}), \\ \zeta_6(\mathbf{s}) &\triangleq \frac{\zeta_5(\mathbf{s})}{3}, & \zeta_9(\mathbf{s}) &\triangleq \frac{\zeta_1(\mathbf{s})}{\zeta_8(\mathbf{s})}. \end{aligned}$$

With these definitions,  $\varphi(\mathbf{s}) = [\mathbf{0}_{1 \times 8} \ 1] \boldsymbol{\zeta}(\mathbf{s})$ , and hence  $\varphi$  is factorable. Note that each factor is defined by applying a simple elementary operation to one or two previous factors. The following definition provides a convenient notation for referring to these individual operations apart from the rest of the function.

**Definition 2.** Let  $\varphi : D \subseteq \mathbb{R}^{n_s} \rightarrow \mathbb{R}^{n_\varphi}$  be a factorable function with factors  $\boldsymbol{\zeta} = (\zeta_1, \dots, \zeta_{n_z})$ . For each  $j \in \{1, \dots, n_z\}$ , let  $\alpha_j : \mathbb{R}^{n_z} \rightarrow \mathbb{R}$  denote the corresponding elementary operation. Specifically:

1. For each  $j \leq n_s$ ,  $\alpha_j(\mathbf{z}) \triangleq z_j$ ,  $\forall \mathbf{z} \in \mathbb{R}^{n_z}$ ;
2. For each  $j > n_s$ ,
  - (a) if  $\zeta_j(\mathbf{s}) = \zeta_a(\mathbf{s}) \odot \zeta_b(\mathbf{s})$ , then  $\alpha_j(\mathbf{z}) \triangleq z_a \odot z_b$ ,  $\forall \mathbf{z} \in \mathbb{R}^{n_z}$ ,
  - (b) if  $\zeta_j(\mathbf{s}) = \beta_j(\zeta_a(\mathbf{s}))$ , then  $\alpha_j(\mathbf{z}) \triangleq \beta_j(z_a)$ ,  $\forall \mathbf{z} \in \mathbb{R}^{n_z}$ .

Note that each  $\alpha_j$  depends on at most two components of  $\mathbf{z}$  (with indices less than  $j$ ) and is only written as a function of the full vector for convenience. With this notation, we always have  $\zeta_j(\mathbf{s}) = \alpha_j(\boldsymbol{\zeta}(\mathbf{s}))$ . The next definition builds the concept of space of factors, which is required in the remainder of the paper.

**Definition 3.** Let  $\varphi : D \subseteq \mathbb{R}^{n_s} \rightarrow \mathbb{R}^{n_\varphi}$  be a factorable function with factors  $\boldsymbol{\zeta} = (\zeta_1, \dots, \zeta_{n_z})$ . Then, the associated *space of factors* is defined by  $\mathcal{Z}(\boldsymbol{\zeta}, D) \triangleq \{\mathbf{z} \in \mathbb{R}^{n_z} : z_i = \zeta_i(\mathbf{s}) \ \forall i \in \{1, 2, \dots, n_z\}, \mathbf{s} \in D\}$ .

Using Definition 3, it is worth mentioning that for every  $\mathbf{s} \in D$ , there exists  $\mathbf{z} \in \mathcal{Z}(\boldsymbol{\zeta}, D)$  such that  $\varphi(\mathbf{s}) = \mathbf{E}_\varphi \mathbf{z}$ , and vice versa. From Definition 2, it also holds that any  $\mathbf{z} \in \mathcal{Z}(\boldsymbol{\zeta}, D)$  satisfies  $z_j = \alpha_j(\mathbf{z})$  for all  $j \in \{1, \dots, n_z\}$ . It is important to note that the factorization of  $\varphi(\mathbf{s})$  is not unique. Additionally, assuming factorability is not very restrictive since any function that can be written explicitly in computer code using a standard math library is factorable.

### 2.3. Convex polytopes and constrained zonotopes

*Convex polytopes* are commonly represented as either the intersection of various halfspaces, or as the convex hull of a collection of vertices. In this work, we use the halfspace representation (H-rep). To facilitate the required manipulations, we use a slightly modified H-rep defined next, which stores linear equality constraints separately from the inequalities.

**Definition 4.** A set  $P \subset \mathbb{R}^n$  is a *convex polytope* in half-space representation if there exists  $(\mathbf{H}_p, \mathbf{k}_p, \mathbf{A}_p, \mathbf{b}_p) \in \mathbb{R}^{n_h \times n} \times \mathbb{R}^{n_h} \times \mathbb{R}^{n_e \times n} \times \mathbb{R}^{n_e}$  such that

$$P = \{\mathbf{x} \in \mathbb{R}^n : \mathbf{H}_p \mathbf{x} \leq \mathbf{k}_p, \mathbf{A}_p \mathbf{x} = \mathbf{b}_p\}. \quad (1)$$

Moreover, *constrained zonotopes* are an extension of zonotopes that include linear equality constraints. This allows CZs to describe arbitrary convex polytopes, while retaining many of the computational advantages of zonotopes in comparison to standard polytope computations.

**Definition 5.** (Scott et al., 2016) A set  $Z \subset \mathbb{R}^n$  is a *constrained zonotope* if there exists  $(\mathbf{G}_z, \mathbf{c}_z, \mathbf{A}_z, \mathbf{b}_z) \in \mathbb{R}^{n \times n_g} \times \mathbb{R}^n \times \mathbb{R}^{n_e \times n_g} \times \mathbb{R}^{n_e}$  such that

$$Z = \{\mathbf{c}_z + \mathbf{G}_z \boldsymbol{\xi} : \|\boldsymbol{\xi}\|_\infty \leq 1, \mathbf{A}_z \boldsymbol{\xi} = \mathbf{b}_z\}. \quad (2)$$

In (1), each inequality is a *half-space*. In (2), each column of  $\mathbf{G}_z$  is a *generator*,  $\mathbf{c}_z$  is the *center*, and  $\mathbf{A}_z \boldsymbol{\xi} = \mathbf{b}_z$  are the *constraints*. We use compact notation  $P = (\mathbf{H}_p, \mathbf{k}_p, \mathbf{A}_p, \mathbf{b}_p)_P$  for convex polytopes in H-rep,  $Z = (\mathbf{G}_z, \mathbf{c}_z, \mathbf{A}_z, \mathbf{b}_z)_{CZ}$  for CZs and  $Z = (\mathbf{G}_z, \mathbf{c}_z)_Z$  for zonotopes. The latter two are referred to as the constrained generator representation (CG-rep) and generator representation (G-rep), respectively. Moreover,  $(\mathbf{H}_p, \mathbf{k}_p, \_, \_)_P$  and  $(\_, \_, \mathbf{A}_p, \mathbf{b}_p)_P$  denote polytopes with only inequality constraints, and only equality constraints, respectively. Note that an interval  $X \in \mathbb{I}\mathbb{R}^n$  can be described in G-rep as  $(\text{diag}(\text{rad}(X)), \text{mid}(X))_Z$ .

Consider sets  $Z, W \subset \mathbb{R}^n$ ,  $Y \subset \mathbb{R}^m$ , and a matrix  $\mathbf{R} \in \mathbb{R}^{m \times n}$ . Define the Cartesian product, linear image, Minkowski sum, and generalized intersection, as  $Z \times W \triangleq \{(\mathbf{z}, \mathbf{w}) : \mathbf{z} \in Z, \mathbf{w} \in W\}$ ,  $\mathbf{R}Z \triangleq \{\mathbf{R}\mathbf{z} : \mathbf{z} \in Z\}$ ,  $Z \oplus W \triangleq \{\mathbf{z} + \mathbf{w} : \mathbf{z} \in Z, \mathbf{w} \in W\}$ , and  $Z \cap_{\mathbf{R}} Y \triangleq \{\mathbf{z} \in Z : \mathbf{R}\mathbf{z} \in Y\}$ , respectively. If  $Z \triangleq (\mathbf{G}_z, \mathbf{c}_z, \mathbf{A}_z, \mathbf{b}_z)_{CZ} \subset \mathbb{R}^n$ ,  $W \triangleq (\mathbf{G}_w, \mathbf{c}_w, \mathbf{A}_w, \mathbf{b}_w)_{CZ} \subset \mathbb{R}^n$ , and  $Y \triangleq (\mathbf{G}_y, \mathbf{c}_y, \mathbf{A}_y, \mathbf{b}_y)_{CZ} \subset \mathbb{R}^m$  are constrained zonotopes, then

$$Z \times W = \left( \begin{bmatrix} \mathbf{G}_z & \mathbf{0} \\ \mathbf{0} & \mathbf{G}_w \end{bmatrix}, \begin{bmatrix} \mathbf{c}_z \\ \mathbf{c}_w \end{bmatrix}, \begin{bmatrix} \mathbf{A}_z & \mathbf{0} \\ \mathbf{0} & \mathbf{A}_w \end{bmatrix}, \begin{bmatrix} \mathbf{b}_z \\ \mathbf{b}_w \end{bmatrix} \right)_{CZ}, \quad (3)$$

$$\mathbf{R}Z = (\mathbf{R}\mathbf{G}_z, \mathbf{R}\mathbf{c}_z, \mathbf{A}_z, \mathbf{b}_z)_{CZ}, \quad (4)$$

$$Z \oplus W = \left( [\mathbf{G}_z \ \mathbf{G}_w], \mathbf{c}_z + \mathbf{c}_w, \begin{bmatrix} \mathbf{A}_z & \mathbf{0} \\ \mathbf{0} & \mathbf{A}_w \end{bmatrix}, \begin{bmatrix} \mathbf{b}_z \\ \mathbf{b}_w \end{bmatrix} \right)_{CZ}, \quad (5)$$

$$Z \cap_{\mathbf{R}} Y = \left( \begin{bmatrix} \mathbf{G}_z & \mathbf{0} \\ \mathbf{0} & \mathbf{A}_y \end{bmatrix}, \begin{bmatrix} \mathbf{c}_z \\ \mathbf{c}_y - \mathbf{R}\mathbf{c}_z \end{bmatrix}, \begin{bmatrix} \mathbf{A}_z & \mathbf{0} \\ \mathbf{0} & \mathbf{A}_y \end{bmatrix}, \begin{bmatrix} \mathbf{b}_z \\ \mathbf{b}_y - \mathbf{R}\mathbf{c}_z \end{bmatrix} \right)_{CZ}. \quad (6)$$

Moreover, define  $B_\infty(\mathbf{A}_z, \mathbf{b}_z) \triangleq \{\boldsymbol{\xi} \in \mathbb{R}^{n_g} : \|\boldsymbol{\xi}\|_\infty \leq 1, \mathbf{A}_z \boldsymbol{\xi} = \mathbf{b}_z\}$ . Then,  $(\mathbf{G}_z, \mathbf{c}_z, \mathbf{A}_z, \mathbf{b}_z)_{CZ} = \mathbf{c}_z \oplus \mathbf{G}_z B_\infty(\mathbf{A}_z, \mathbf{b}_z)$  holds, and

$(\mathbf{G}_z, \mathbf{c}_z)_Z = \mathbf{c}_z \oplus \mathbf{G}_z \mathbf{B}_\infty^n$ . Additionally, if  $P \triangleq (\mathbf{H}_p, \mathbf{k}_p, \mathbf{A}_p, \mathbf{b}_p)_P \subset \mathbb{R}^n$  and  $Q \triangleq (\mathbf{H}_q, \mathbf{k}_q, \mathbf{A}_q, \mathbf{b}_q)_Q \subset \mathbb{R}^n$ , then

$$P \cap Q = \left( \begin{bmatrix} \mathbf{H}_p \\ \mathbf{H}_q \end{bmatrix}, \begin{bmatrix} \mathbf{k}_p \\ \mathbf{k}_q \end{bmatrix}, \begin{bmatrix} \mathbf{A}_p \\ \mathbf{A}_q \end{bmatrix}, \begin{bmatrix} \mathbf{b}_p \\ \mathbf{b}_q \end{bmatrix} \right)_P. \quad (7)$$

Efficient methods to enclose a CZ by another one with fewer generators and constraints are available in [Scott et al. \(2016\)](#). In addition, the interval hull of a CZ  $Z \subset \mathbb{R}^n$ , denoted as  $\square Z \in \mathbb{I}\mathbb{R}^n$ , can be computed by solving  $2n$  linear programs ([Scott et al., 2016](#); [Rego et al., 2018](#)).

Finally, the following proposition provides a method to obtain a CZ describing the exact intersection of a CZ and a convex polytope in H-rep.

**Proposition 1.** ([Rego et al., 2024](#)) Let  $Z = (\mathbf{G}_z, \mathbf{c}_z, \mathbf{A}_z, \mathbf{b}_z)_{\text{CZ}} \subset \mathbb{R}^n$  be a constrained zonotope and  $P \triangleq (\mathbf{H}_p, \mathbf{k}_p, \mathbf{A}_p, \mathbf{b}_p)_P \subset \mathbb{R}^n$  be a convex polytope in H-rep with  $n_h$  half-spaces. Choose any  $\boldsymbol{\sigma} \in \mathbb{R}^{n_h}$  satisfying  $\boldsymbol{\sigma} \leq \mathbf{H}_p \mathbf{z}$ ,  $\forall \mathbf{z} \in Z$ , and define  $\mathbf{G}_q \triangleq \frac{1}{2} \text{diag}(\mathbf{k}_p - \boldsymbol{\sigma})$ , and  $\mathbf{c}_q \triangleq \frac{1}{2}(\mathbf{k}_p + \boldsymbol{\sigma})$ . Then,

$$Z \cap P = \left( \begin{bmatrix} \mathbf{G}_z & \mathbf{0} \\ \mathbf{H}_p & \mathbf{G}_z \end{bmatrix}, \begin{bmatrix} \mathbf{c}_z \\ \mathbf{c}_q - \mathbf{H}_p \mathbf{c}_z \end{bmatrix}, \begin{bmatrix} \mathbf{A}_z & \mathbf{0} \\ \mathbf{A}_p & \mathbf{G}_z \end{bmatrix}, \begin{bmatrix} \mathbf{b}_z \\ \mathbf{b}_p - \mathbf{A}_p \mathbf{c}_z \end{bmatrix} \right)_{\text{CZ}}. \quad (8)$$

**Remark 1.** To calculate  $\boldsymbol{\sigma} \in \mathbb{R}^{n_h}$  needed in Proposition 1, satisfying  $\boldsymbol{\sigma} \leq \mathbf{H}_p \mathbf{z}$  for all  $\mathbf{z} \in Z$ , let  $\check{Z} \triangleq (\mathbf{G}_z, \mathbf{c}_z)_Z$  be the zonotope obtained by neglecting the constraints of  $Z$ . It holds that  $Z \subset \check{Z}$ . In this work, we use a valid choice of  $\boldsymbol{\sigma}$  obtained by the lower bound of the interval computed by  $\square(\mathbf{H}\check{Z})$ . This procedure does not require the solution of linear programs since the argument  $\mathbf{H}\check{Z}$  is a zonotope.

#### 2.4. Problem formulation

Consider the nonlinear discrete-time system

$$\mathbf{x}_k = \mathbf{f}(\mathbf{x}_{k-1}, \mathbf{w}_{k-1}, \mathbf{u}_{k-1}), \quad k \geq 1, \quad (9a)$$

$$\mathbf{y}_k = \mathbf{g}(\mathbf{x}_k, \mathbf{v}_k), \quad k \geq 0, \quad (9b)$$

where  $\mathbf{x}_k \in \mathbb{R}^{n_x}$  is the system state,  $\mathbf{u}_k \in \mathbb{R}^{n_u}$  is a known input,  $\mathbf{y}_k \in \mathbb{R}^{n_y}$  is the measured output, and  $(\mathbf{w}_k, \mathbf{v}_k) \in \mathbb{R}^{n_w+n_v}$  are bounded uncertainties. The functions  $\mathbf{f} : \mathbb{R}^{n_x} \times \mathbb{R}^{n_w} \times \mathbb{R}^{n_u} \rightarrow \mathbb{R}^{n_x}$  and  $\mathbf{g} : \mathbb{R}^{n_x} \times \mathbb{R}^{n_v} \times \mathbb{R}^{n_u} \rightarrow \mathbb{R}^{n_y}$  are assumed to be factorable. The initial condition and uncertainties are assumed to be bounded by  $(\mathbf{x}_0, \mathbf{w}_k, \mathbf{v}_k) \in X_0 \times W \times V$ , where  $X_0$ ,  $W$ , and  $V$  are known convex polytopes.

The objective of this work is to obtain convex enclosures  $\hat{X}_k$  of all the possible states that are consistent with the initial set  $X_0$ , the uncertainty sets  $W$  and  $V$ , the dynamics (9a) and all measurements (9b) up to time  $k$ . For  $k = 0$ ,

$$\hat{X}_0 \supseteq \{\mathbf{x}_0 \in X_0 : \mathbf{g}(\mathbf{x}_0, \mathbf{v}_0) = \mathbf{y}_0, \mathbf{v}_0 \in V\}, \quad (10)$$

whereas, for  $k \geq 1$ , this is accomplished using the recursive approach

$$\hat{X}_k \supseteq \{\mathbf{x}_k = \mathbf{f}(\mathbf{x}_{k-1}, \mathbf{w}_{k-1}, \mathbf{u}_{k-1}) \in \mathbb{R}^{n_x} : \mathbf{y}_k = \mathbf{g}(\mathbf{x}_k, \mathbf{v}_k), (\mathbf{x}_{k-1}, \mathbf{w}_{k-1}, \mathbf{v}_k) \in \hat{X}_{k-1} \times W \times V\}. \quad (11)$$

With  $X_0$  and  $W$  described as CZs, the key step consists of propagating constrained zonotopes through the nonlinear function  $\mathbf{f}$ , in addition to refining CZ enclosures using the nonlinear equality constraints  $\mathbf{g}(\mathbf{x}_k, \mathbf{v}_k) = \mathbf{y}_k$ .

**Remark 2.** The trajectories of real processes often satisfy solution invariants such as conservation of mass or energy. This information consists of equality constraints that can be used to refine reachable sets and estimated enclosures ([Yang & Scott, 2018a](#); [Rego et al., 2021](#)). Invariants of the form  $\mathbf{h}(\mathbf{x}_k, \mathbf{d}_k) = \mathbf{0}$ , can be included in (11) and (10) straightforwardly, where  $\mathbf{h} : \mathbb{R}^{n_x} \times \mathbb{R}^{n_d} \rightarrow \mathbb{R}^{n_h}$  is assumed to be factorable, and  $\mathbf{d}_k \in \mathbb{R}^{n_d}$  is a bounded uncertainty. Such equality constraints can be interpreted as virtual measurement equations, and therefore can be included in (9b) with measurement  $\mathbf{0}$ .

### 3. Lifted convex polytope enclosing the image of a nonlinear function over an interval

This section describes the core of the proposed state estimation method, which consists of a methodology to obtain a convex polytope enclosing the space of factors of a nonlinear factorable function with interval domain. Since each factor is given by an elementary function of the other factors, obtaining this enclosure is considerably easier than directly enclosing the image of the nonlinear function. This enclosure is also less conservative for the same reason. Later steps of the proposed method deal with computing the projection of this enclosure onto the image of the nonlinear function.

Consider a factorable function  $\boldsymbol{\varphi} : S \subset \mathbb{R}^{n_s} \rightarrow \mathbb{R}^{n_\varphi}$ , with interval domain  $S \in \mathbb{I}\mathbb{R}^{n_s}$ , and factors  $\boldsymbol{\zeta} = (\zeta_1, \dots, \zeta_{n_\zeta})$ , following Definition 1, such that  $\boldsymbol{\varphi}(\mathbf{s}) = \mathbf{E}_\varphi \boldsymbol{\zeta}(\mathbf{s})$  for all  $\mathbf{s} \in S$ . The objective is to compute a convex polytope  $P_\varphi \in \mathbb{R}^{n_\varphi}$  enclosing the space of factors  $\mathcal{Z}(\boldsymbol{\zeta}, S)$ . This polytope satisfies  $\{\boldsymbol{\varphi}(\mathbf{s}) : \mathbf{s} \in S\} = \{\mathbf{E}_\varphi \mathbf{z} : \mathbf{z} \in \mathcal{Z}(\boldsymbol{\zeta}, S)\} \subseteq \{\mathbf{E}_\varphi \mathbf{z} : \mathbf{z} \in P_\varphi\}$ .

**Proposition 2.** Let  $\boldsymbol{\varphi} : S \subset \mathbb{R}^{n_s} \rightarrow \mathbb{R}^{n_\varphi}$  be a factorable function with interval domain  $S \in \mathbb{I}\mathbb{R}^{n_s}$ , and factors  $\boldsymbol{\zeta} = (\zeta_1, \dots, \zeta_{n_\zeta})$ , following Definition 1. Consider an interval  $Z \in \mathbb{I}\mathbb{R}^{n_\zeta}$  satisfying  $\boldsymbol{\zeta}(\mathbf{s}) \in Z$  for all  $\mathbf{s} \in S$ . Moreover, for each  $j > n_s$ ,

- Let  $\alpha_j : \mathbb{R}^{n_\zeta} \rightarrow \mathbb{R}$  according to Definition 2,
- Compute a halfspace enclosure  $Q_j \supseteq \{\mathbf{z} \in Z : z_j = \alpha_j(\mathbf{z})\}$ .

Then,  $\mathcal{Z}(\boldsymbol{\zeta}, S) \subseteq P_\varphi$ , where

$$P_\varphi \triangleq \bigcap_{j=n_s+1}^{n_\zeta} Q_j. \quad (12)$$

*Proof.* By assumption, any  $\mathbf{s} \in S \implies \boldsymbol{\zeta}(\mathbf{s}) \in Z$ . Therefore, for any  $\mathbf{s} \in S$  and all  $j \in \{1, \dots, n_\zeta\}$ , there exists  $\mathbf{z} \in Z$  such that  $z_j = \zeta_j(\mathbf{s}) = \alpha_j(\mathbf{z})$ . Consequently, for any  $\mathbf{z} \in \mathcal{Z}(\boldsymbol{\zeta}, S)$  (see Definition 3),  $\mathbf{z} \in \bigcap_{j=1}^{n_\zeta} \{\mathbf{z} \in Z : z_j = \alpha_j(\mathbf{z})\} \subset \bigcap_{j=n_s+1}^{n_\zeta} Q_j \triangleq P_\varphi$ , with  $Q_j$  defined as in the statement of the proposition. Finally, this implies that any  $\mathbf{z} \in \mathcal{Z}(\boldsymbol{\zeta}, S)$  satisfies  $\mathbf{z} \in P_\varphi$ , which proves the proposition.  $\blacksquare$

**Corollary 1.** Let  $\varphi : S \subset \mathbb{R}^{n_s} \rightarrow \mathbb{R}^{n_\varphi}$  be a factorable function with interval domain  $S \in \mathbb{I}\mathbb{R}^{n_s}$ , and factors  $\zeta = (\zeta_1, \dots, \zeta_{n_\zeta})$ , following Definition 1, such that  $\varphi(\mathbf{s}) = \mathbf{E}_\varphi \zeta(\mathbf{s})$ . Let  $P_\varphi$  be the polyhedral enclosure computed as in Proposition 2. Then,  $\{\varphi(\mathbf{s}) : \mathbf{s} \in S\} \subseteq \{\mathbf{E}_\varphi \mathbf{z} : \mathbf{z} \in P_\varphi\}$ .

*Proof.* From Definition 3, for any  $\mathbf{s} \in S$ , there exists  $\mathbf{z} \in \mathcal{Z}(\zeta, S)$  such that  $\varphi(\mathbf{s}) = \mathbf{E}_\varphi \mathbf{z}$ . By Proposition 2, since  $\mathcal{Z}(\zeta, S) \subseteq P_\varphi$ , it is also true that  $\mathbf{z} \in P_\varphi$ . Therefore, for any  $\mathbf{s} \in S$ ,  $\varphi(\mathbf{s}) \in \{\mathbf{E}_\varphi \mathbf{z} : \mathbf{z} \in P_\varphi\}$ , which proves the corollary. ■

**Remark 3.** In our implementation, a valid choice for the interval  $Z$  required in Proposition 2 is computed as follows. For  $j = 1, \dots, n_s$ ,  $Z_j \triangleq S_j \in \mathbb{I}\mathbb{R}$ . For  $j > n_s$ , the sequence of intervals  $Z_j \in \mathbb{I}\mathbb{R}$  is obtained recursively using interval arithmetic, satisfying either  $\{z_a \odot z_b : (z_a, z_b) \in Z_a \times Z_b\} \subseteq Z_j$ ,  $a, b < j$ , or  $\{\beta_j(z_a) : z_a \in Z_a\} \subseteq Z_j$ ,  $a < j$ , according to each  $\alpha_j$  as in Definition 2.

The lifted polyhedral enclosure computed in Proposition 2 is the core of the state estimation method proposed in this paper, where the projection  $\{\mathbf{E}_\varphi \mathbf{z} : \mathbf{z} \in P_\varphi\}$  discussed in Corollary 1 allows for enclosing the image of the nonlinear function  $\varphi$  over  $S$ . The main challenge consists in obtaining the halfspace enclosures  $Q_j \supseteq \{\mathbf{z} \in Z : z_j = \alpha_j(\mathbf{z})\}$  for the factorable representation of  $\varphi$ . Once these are known, the intersection (12) is computed trivially using (7). The following subsections illustrate how such halfspace enclosures can be easily obtained for some common elementary operations.

### 3.1. Arithmetic operations

Let  $z_j = \alpha_j(\mathbf{z}) \triangleq z_a \odot z_b$  with  $a, b < j$ ,  $j > n_s$  and  $\odot \in \{+, -, \times, /\}$ ,  $z_a \in Z_a \triangleq [z_a^L, z_a^U]$ , and  $z_b \in Z_b \triangleq [z_b^L, z_b^U]$ . For these four arithmetic operations, the halfspace enclosures  $Q_j$  can be obtained as explained below.

*Addition.*  $z_j = z_a + z_b$ . An exact halfspace enclosure is obtained by rearranging it as  $-z_a - z_b + z_j = 0$ . This gives  $Q_j = \{\mathbf{z} : \mathbf{r}_+ \mathbf{z} = 0\} = (\_, \_, \mathbf{r}_+, 0)_P$ , where  $\mathbf{r}_+$  is a row vector of zeros, except for the  $a$ th,  $b$ th, and  $j$ th columns, which are  $-1$ ,  $-1$ , and  $1$ , respectively.

*Subtraction.*  $z_j = z_a - z_b$ . Analogously to addition, an exact halfspace enclosure is given by  $Q_j = (\_, \_, \mathbf{r}_-, 0)_P$ , where  $\mathbf{r}_-$  is a row vector of zeros, except for the  $a$ th,  $b$ th, and  $j$ th columns, which are  $-1$ ,  $1$ , and  $1$ , respectively.

*Multiplication.*  $z_j = z_a z_b$ . The halfspace enclosure  $Q_j$  is obtained by rearranging the four inequalities derived from the McCormick relaxations for the bilinear function  $z_j = z_a z_b$ , which are (McCormick, 1976)

$$\begin{aligned} z_j &\geq z_a^L z_b + z_a z_b^L - z_a^L z_b^L, \\ z_j &\geq z_a^U z_b + z_a z_b^U - z_a^U z_b^U, \\ z_j &\leq z_a^L z_b + z_a z_b^U - z_a^L z_b^U, \\ z_j &\leq z_a^U z_b + z_a z_b^L - z_a^U z_b^L. \end{aligned}$$

*Division.*  $z_j = \frac{z_a}{z_b}$ . The halfspace enclosure  $Q_j$  is obtained by rewriting  $z_j = \frac{z_a}{z_b}$  as  $z_a = z_b z_j$  and applying the multiplication enclosure accordingly.

**Remark 4.** For the case of arithmetic operations with constant parameters, such as  $z_j = q z_a$ , with  $q \in \mathbb{R}$  known, special halfspace enclosures  $Q_j$  can be obtained using simpler representations.

### 3.2. Univariate functions

Let  $z_j = \alpha_j(\mathbf{z}) \triangleq \beta_j(z_a)$ , where  $a < j$ ,  $j > n_s$ ,  $z_a \in Z_a \triangleq [z_a^L, z_a^U]$ , and  $\beta_j$  is an intrinsic univariate function in the library  $\mathcal{L}$ . For all such functions, we assume that convex and concave relaxations on  $Z_a$  can be readily constructed. Specifically, given any  $Z_a \in \mathbb{I}\mathbb{R}$ , we have convex and concave functions  $\beta_j^{\text{CV}} : Z_a \rightarrow \mathbb{R}$  and  $\beta_j^{\text{CC}} : Z_a \rightarrow \mathbb{R}$ , respectively, such that

$$\beta_j^{\text{CV}}(z_a) \leq \beta_j(z_a) \leq \beta_j^{\text{CC}}(z_a), \quad \forall z_a \in Z_a. \quad (13)$$

Such relaxations are tabulated for a wide variety of common univariate functions in many global optimization references; see e.g. Chapter 2 in Scott (2012).

Using these functions, we seek to compute a polyhedral enclosure of the form  $Q_j = Q_j^{\text{CV}} \cap Q_j^{\text{CC}}$ , where

$$Q_j^{\text{CV}} \supseteq \{\mathbf{z} \in \mathbb{R}^{n_z} : z_j \geq \beta_j^{\text{CV}}(z_a), z_a \in Z_a\}, \quad (14)$$

$$Q_j^{\text{CC}} \supseteq \{\mathbf{z} \in \mathbb{R}^{n_z} : z_j \leq \beta_j^{\text{CC}}(z_a), z_a \in Z_a\}. \quad (15)$$

Then, it holds that  $Q_j \supseteq \{\mathbf{z} \in \mathbb{R}^{n_z} : z_j = \beta_j(z_a), z_a \in Z_a\}$ , as desired. Since  $\beta_j^{\text{CV}}$  is convex and  $\beta_j^{\text{CC}}$  is concave, the inequalities in (14)–(15) remain true if  $\beta_j^{\text{CV}}$  and  $\beta_j^{\text{CC}}$  are replaced by their linearizations at any point in  $Z_a$ . Therefore, our general strategy is to define  $Q_j^{\text{CV}}$  and  $Q_j^{\text{CC}}$  in terms of linearizations of  $\beta_j^{\text{CV}}$  and  $\beta_j^{\text{CC}}$  at a set of reference points. In many cases, these functions are linear, so no linearization is needed. Otherwise, we use linearizations at  $z_a^L$ ,  $z_a^M$ , and  $z_a^U$ . A few specific examples are given below.

*Exponential.*  $z_j = e^{z_a}$ . In this case,  $\beta_j(z_a)$  is convex, so  $\beta_j^{\text{CV}} = \beta_j$ . Thus,  $Q_j^{\text{CV}}$  is obtained by linearizing  $\beta_j$  at  $z_a^L$ ,  $z_a^M$ , and  $z_a^U$ , leading to the inequalities  $z_j \geq e^{z_a^L}(z_a - z_a^L) + e^{z_a^L}$ ,  $z_j \geq e^{z_a^M}(z_a - z_a^M) + e^{z_a^M}$ , and  $z_j \geq e^{z_a^U}(z_a - z_a^U) + e^{z_a^U}$ . The concave relaxation on  $Z_a$  is the secant  $\beta_j^{\text{CC}}(z_a) = \left( \frac{e^{z_a^U} - e^{z_a^L}}{z_a^U - z_a^L} \right) (z_a - z_a^L) + e^{z_a^L}$ . Thus,  $Q_j^{\text{CC}}$  is defined by the single inequality  $z_j \leq \beta_j^{\text{CC}}(z_a)$ .

*Logarithm.*  $z_j = \ln(z_a)$ . In this case,  $\beta_j(z_a)$  is concave, so  $\beta_j^{\text{CC}} = \beta_j$ . Thus,  $Q_j^{\text{CC}}$  is obtained by linearizing  $\beta_j$  at  $z_a^L$ ,  $z_a^M$ , and  $z_a^U$ , leading to  $z_j \leq \frac{1}{z_a^L}(z_a - z_a^L) + \ln(z_a^L)$ ,  $z_j \leq \frac{1}{z_a^M}(z_a - z_a^M) + \ln(z_a^M)$ , and  $z_j \leq \frac{1}{z_a^U}(z_a - z_a^U) + \ln(z_a^U)$ . The convex relaxation on  $Z_a$  is the secant  $\beta_j^{\text{CV}}(z_a) = \left( \frac{\ln(z_a^U) - \ln(z_a^L)}{z_a^U - z_a^L} \right) (z_a - z_a^L) + \ln(z_a^L)$ . Thus,  $Q_j^{\text{CV}}$  is defined by the single inequality  $z_j \geq \beta_j^{\text{CV}}(z_a)$ .

*Even integer power.*  $z_j = z_a^q$  with  $q$  an even integer. In this case,  $\beta_j(z_a)$  is convex, so  $\beta_j^{\text{CV}} = \beta_j$ . Thus,  $Q_j^{\text{CV}}$  is obtained by linearizing  $\beta_j$  at  $z_a^L$ ,  $z_a^M$ , and  $z_a^U$ , leading to the inequalities  $z_j \geq q(z_a^L)^{(q-1)}(z_a - z_a^L) + (z_a^L)^q$ ,  $z_j \geq q(z_a^M)^{(q-1)}(z_a - z_a^M) + (z_a^M)^q$ , and  $z_j \geq q(z_a^U)^{(q-1)}(z_a - z_a^U) + (z_a^U)^q$ . The concave relaxation on  $Z_a$  is the secant  $\beta_j^{\text{CC}}(z_a) = \left( \frac{(z_a^U)^q - (z_a^L)^q}{z_a^U - z_a^L} \right) (z_a - z_a^L) + (z_a^L)^q$ . Thus,  $Q_j^{\text{CC}}$  is defined by the single inequality  $z_j \leq \beta_j^{\text{CC}}(z_a)$ .

*Odd integer power.*  $z_j = z_a^q$  with  $q$  an odd integer. In this case,  $\beta_j(z_a)$  is concave for  $z_a \leq 0$ , and convex for  $z_a \geq 0$ . Therefore, for  $z_a^L \leq 0$ , the enclosures  $Q_j^{\text{CV}}$  and  $Q_j^{\text{CC}}$  are obtained analogously to the logarithm, while for  $z_a^L \geq 0$ , the enclosures they are obtained analogously to the even integer power. If  $0 \in [z_a^L, z_a^U]$ , the procedure is significantly more involved and can be found in Chapter 2 of Scott (2012).

*Sine.*  $z_j = \sin(z_a)$ . In this case,  $\beta_j(z_a)$  is a periodic function, piecewise alternating between convexity and concavity. For this reason, the interval  $[z_a^L, z_a^U]$  is first partitioned according to the conditions found in Chapter 2 of Scott (2012), with  $Q_j^{\text{CV}}$  and  $Q_j^{\text{CC}}$  given by the intersection of multiple halfspaces obtained either from the secant, or from the linearization of  $\beta_j$  around the respective endpoints and midpoint, for each one of the sub-regions involved. Further details can be found in Appendix A.

*Cosine.*  $z_j = \cos(z_a)$ . In this case, we use the fact  $\cos(z_a) = \sin(z_a + \frac{\pi}{2})$ . The halfspaces  $Q_j^{\text{CV}}$  and  $Q_j^{\text{CC}}$  are obtained by decomposing  $\cos(z_a) = \sin(z_a + \frac{\pi}{2})$  into  $z_b \triangleq z_a + \frac{\pi}{2}$  and  $z_j = \sin(z_b)$ , and using the respective methods for the addition and sine functions.

Figure 1 illustrates an example of halfspace enclosure  $Q_j$ , for  $z_j = \sin(z_a)$ , with  $z_a \in [-\frac{3\pi}{4}, \pi]$ . As it can be noticed,  $Q_j$  approximates the convex hull of the image of the sine function by a tight convex polytope with limited complexity. Enabling the computation of polyhedral enclosures for trigonometric functions is an important contribution with respect to the literature, in special to our previous work (Rego et al., 2024). These functions often appear in the dynamics of industrial and robotics applications, and therefore the computation of these enclosures is essential for reachability analysis and state estimation of such systems.

#### 4. State estimation

This section presents a new method for computing constrained zonotope enclosures  $\hat{X}_k$  satisfying (11) using polyhedral relaxations, denoted as CZPR. In accordance to the set-based state estimation literature, we refer to the computation of this enclosure as the *prediction-update step*, since it combines in one step the propagation of the previous enclosure  $\hat{X}_{k-1}$  and  $W$  through the nonlinear dynamics (9a) (prediction step), and the refinement of the propagated set using the measurement  $\mathbf{y}_k$ , the uncertainty set  $V$ , and the measurement equation (9b) (update step). Likewise, the proposed methodology is an extension of the reachability enclosure method developed in Rego et al. (2024) to take into account available nonlinear measurements.

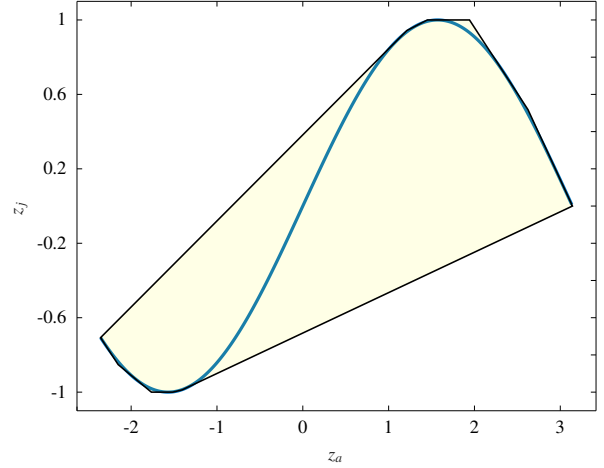


Figure 1: An example of halfspace enclosure  $Q_j \supset \{(z_j, z_a) \in \mathbb{R} \times Z_a : z_j = \sin(z_a)\}$  (yellow), where  $Z_a = [-\frac{3\pi}{4}, \pi]$ , along with the exact set  $\{(z_j, z_a) \in \mathbb{R} \times Z_a : z_j = \sin(z_a)\}$  (solid blue line).

Let the previous estimated set  $\hat{X}_{k-1} \ni \mathbf{x}_{k-1}$  be a constrained zonotope. Using the ideas developed in Section 3, the main objective is to compute an enclosure  $\hat{X}_k$  of  $\underline{X}_k$ , where

$$\begin{aligned} \underline{X}_k &\triangleq \{\mathbf{x}_k = \mathbf{f}(\mathbf{x}_{k-1}, \mathbf{w}_{k-1}, \mathbf{u}_{k-1}) : \mathbf{y}_k = \mathbf{g}(\mathbf{x}_k, \mathbf{v}_k), \\ &\quad (\mathbf{x}_{k-1}, \mathbf{w}_{k-1}, \mathbf{v}_k) \in \hat{X}_{k-1} \times W \times V\}. \end{aligned} \quad (16)$$

This is achieved in a few steps, as follows.

Define the composite function  $\ell : \mathbb{R}^{n_x} \times \mathbb{R}^{n_w} \times \mathbb{R}^{n_v} \times \mathbb{R}^{n_u} \rightarrow \mathbb{R}^{n_y}$ ,  $\ell(\mathbf{x}_{k-1}, \mathbf{w}_{k-1}, \mathbf{v}_k, \mathbf{u}_{k-1}) \triangleq \mathbf{g}(\mathbf{f}(\mathbf{x}_{k-1}, \mathbf{w}_{k-1}, \mathbf{u}_{k-1}), \mathbf{v}_k)$ . Since both  $\mathbf{f}$  and  $\mathbf{g}$  are factorable,  $\ell$  is also factorable. Let  $\zeta = \{\zeta_1, \dots, \zeta_{n_z}\}$  be the factors of  $\ell$ , and let  $\mathbf{s} \triangleq (\mathbf{x}_{k-1}, \mathbf{w}_{k-1}, \mathbf{v}_k)$  be the input. Moreover, define  $S \triangleq \hat{X}_{k-1} \times W \times V$ . Then, from Definition 1, for any  $\mathbf{s} \in S$  there exists  $\mathbf{E}_\ell$  such that  $\ell(\mathbf{s}, \mathbf{u}_{k-1}) = \mathbf{E}_\ell \zeta(\mathbf{s}, \mathbf{u}_{k-1})$ . By the construction of  $\ell$ , it is also true that  $\mathbf{f}$  can be described in terms of the factors  $\zeta$ . As such, there exists  $\mathbf{E}_f$  such that  $\mathbf{f}(\mathbf{s}, \mathbf{u}_{k-1}) = \mathbf{E}_f \zeta(\mathbf{s}, \mathbf{u}_{k-1})$ . Note that, since  $\mathbf{u}_{k-1}$  is known, it is a constant parameter in the factorable representations of both  $\mathbf{f}$  and  $\ell$ . Therefore, it is not needed to be included in  $\mathbf{s}$ .

From the definitions above, the estimation problem can be rewritten in terms of the computation of an enclosure of

$$\underline{X}_k = \{\mathbf{f}(\mathbf{s}, \mathbf{u}_{k-1}) : \ell(\mathbf{s}, \mathbf{u}_{k-1}) = \mathbf{y}_k, \mathbf{s} \in S\}. \quad (17)$$

The problem is first addressed in terms of the interval  $\square S = \square(\hat{X}_{k-1}, W, V)$ , for which a polyhedron enclosure  $P_\ell$  is obtained according to Proposition 2. This enclosure satisfies  $\mathcal{Z}(\zeta, \square S) \subseteq P_\ell$ . This polyhedron is then refined with the measurement  $\mathbf{y}_k$  by incorporating the equality constraint  $\ell(\mathbf{s}, \mathbf{u}_{k-1}) = \mathbf{y}_k$  through the intersection of  $P_\ell$  with  $\{\mathbf{z} \in \mathbb{R}^{n_z} : \mathbf{E}_\ell \mathbf{z} = \mathbf{y}_k\}$  (using (7)).

Note that by using an interval enclosure of  $(\hat{X}_{k-1}, W, V)$  as input, any previous dependencies between states is lost in the computation of  $P_\ell$ . This information is later recovered through intersection with the original CZ input  $(\hat{X}_{k-1}, W, V)$  (using (8)). An important property of this operation is that it results in a CZ, which allows it to be easily projected onto the image of  $\mathbf{f}$

by means of  $\mathbf{E}_f$  (using (4)). The following proposition presents the valid estimated enclosure  $\hat{X}_k$  based on these steps.

**Proposition 3.** Consider  $\underline{X}_k, \hat{X}_{k-1}, W, V, \mathbf{u}_{k-1}, \mathbf{y}_k, \ell, \zeta, \mathbf{E}_f, \mathbf{E}_\ell, \mathbf{s}$ , and  $S$  as defined above. Let  $P_y \triangleq (\_, \_, \mathbf{E}_\ell, \mathbf{y}_k)_P$ . For the interval domain  $\square S$  and factors  $\zeta$ , compute a halfspace enclosure  $P_\ell$  as in Proposition 2. Let  $\tilde{Z}$  denote the last  $n_z - (n_x + n_w + n_v)$  factors of  $\ell$ , and consider a set  $\tilde{Z}$  such that  $\tilde{\zeta}(\mathbf{s}, \mathbf{u}_{k-1}) \in \tilde{Z}$  for all  $\mathbf{s} \in S$ . Then,  $\underline{X}_k \subseteq \hat{X}_k$ , where

$$\hat{X}_k \triangleq \mathbf{E}_f((\hat{X}_{k-1} \times W \times V \times \tilde{Z}) \cap (P_\ell \cap P_y)). \quad (18)$$

*Proof.* By Proposition 2, it is true that  $\mathcal{Z}(\zeta, \square S) \subseteq P_\ell$ . Then, for any  $\mathbf{s} \in \square S$ , there exists  $\mathbf{z} \in P_\ell$  such that both  $\mathbf{f}(\mathbf{s}, \mathbf{u}_{k-1}) = \mathbf{E}_f \mathbf{z}$  and  $\ell(\mathbf{s}, \mathbf{u}_{k-1}) = \mathbf{E}_\ell \mathbf{z}$ . This implies that for any  $\mathbf{s} \in \square S$  such that  $\ell(\mathbf{s}, \mathbf{u}_{k-1}) = \mathbf{y}_k$ , there exists  $\mathbf{z} \in P_\ell$  such that  $\mathbf{E}_\ell \mathbf{z} = \mathbf{y}_k$ . By the definition of  $P_y$ , this is equivalent to  $\mathbf{z} \in (P_\ell \cap P_y)$ .

By (17), for any  $\mathbf{s} \in S$  such that  $\mathbf{f}(\mathbf{s}, \mathbf{u}_{k-1}) \in \underline{X}_k, \ell(\mathbf{s}, \mathbf{u}_{k-1}) = \mathbf{y}_k$ . From the facts above and  $\mathbf{s} \in S \implies \mathbf{s} \in \square S$ , then  $\mathbf{f}(\mathbf{s}, \mathbf{u}_{k-1}) \in \underline{X}_k \implies \mathbf{f}(\mathbf{s}, \mathbf{u}_{k-1}) \in \{\mathbf{E}_f \mathbf{z} : \mathbf{z} \in (P_\ell \cap P_y)\}$ . Additionally, by the definition of  $\tilde{Z}$ , we have  $\mathbf{s} \in S \implies (\mathbf{s}, \tilde{\zeta}(\mathbf{s}, \mathbf{u}_{k-1})) = \zeta(\mathbf{s}, \mathbf{u}_{k-1}) \in S \times \tilde{Z}$ . Then, it is also true that  $\mathbf{f}(\mathbf{s}, \mathbf{u}_{k-1}) \in \underline{X}_k \implies \mathbf{f}(\mathbf{s}, \mathbf{u}_{k-1}) \in \{\mathbf{E}_f \mathbf{z} : \mathbf{z} \in (P_\ell \cap P_y), \mathbf{z} \in S \times \tilde{Z}\}$ . Since  $S = \hat{X}_{k-1} \times W \times V$  by definition, then  $\mathbf{f}(\mathbf{s}, \mathbf{u}_{k-1}) \in \underline{X}_k \implies \mathbf{f}(\mathbf{s}, \mathbf{u}_{k-1}) \in \hat{X}_k$ , with  $\hat{X}_k$  given by (18), which proves the proposition. ■

**Remark 5.** In some applications, one may be interested in an enclosure for  $\{\mathbf{f}(\mathbf{x}_{k-1}, \mathbf{w}_{k-1}, \mathbf{u}_{k-1}) : (\mathbf{x}_{k-1}, \mathbf{w}_{k-1}) \in \hat{X}_{k-1} \times W\}$ , also called the predicted set (or reachable set), denoted as  $\tilde{X}_k$ . This enclosure can be obtained straightforwardly based on Propositions 2 and 3. Let  $\delta = \{\delta_1, \dots, \delta_{n_\delta}\}$  be the factors of  $\mathbf{f}$ , and compute a halfspace enclosure  $P_f$  as in Proposition 2, satisfying  $\mathcal{Z}(\delta, \square(\hat{X}_{k-1} \times W)) \subseteq P_f$ . Let  $\mathbf{s} \triangleq (\mathbf{x}_{k-1}, \mathbf{w}_{k-1})$ , let  $\tilde{\delta}$  denote the last  $n_\delta - (n_x + n_w)$  factors of  $\mathbf{f}$ , and consider a set  $\tilde{\Delta}$  satisfying  $\tilde{\delta}(\mathbf{s}, \mathbf{u}_{k-1}) \in \tilde{\Delta}$  for all  $\mathbf{s} \in \hat{X}_{k-1} \times W$ . Then,  $\tilde{X}_k = \mathbf{E}_f((\hat{X}_{k-1} \times W \times \tilde{\Delta}) \cap P_f)$ .

**Remark 6.** For  $k = 0$ , the initial set  $\hat{X}_0$  satisfying (10) can be obtained similarly to Proposition 3, by using the factorable representation of  $\mathbf{g}$  instead of the composite function  $\ell$ . Consider  $\mathbf{s} \triangleq (\mathbf{x}_0, \mathbf{v}_0)$ . Let  $\gamma = \{\gamma_1, \dots, \gamma_{n_\gamma}\}$  be the factors of  $\mathbf{g}$ , such that  $\mathbf{g}(\mathbf{s}) = \mathbf{E}_g \gamma(\mathbf{s})$ . Compute a halfspace enclosure  $P_g$  as in Proposition 2, satisfying  $\mathcal{Z}(\gamma, \square(X_0 \times V)) \subseteq P_g$ , and define  $P_y \triangleq (\_, \_, \mathbf{E}_g, \mathbf{y}_0)_P$ . Let  $\tilde{\gamma}$  denote the last  $n_\gamma - (n_x + n_v)$  factors of  $\mathbf{g}$ , and consider a set  $\tilde{\Gamma}$  satisfying  $\tilde{\gamma}(\mathbf{s}) \in \tilde{\Gamma}$  for all  $\mathbf{s} \in X_0 \times V$ . Then,  $\{\mathbf{x}_0 \in X_0 : \mathbf{y}_0 = \mathbf{g}(\mathbf{x}_0, \mathbf{v}_0), \mathbf{v}_0 \in V\} \subseteq \hat{X}_0$ , where  $\hat{X}_0 \triangleq \mathbf{E}_x((\hat{X}_0 \times V \times \tilde{\Gamma}) \cap (P_g \cap P_y))$ , with  $\mathbf{E}_x \triangleq [\mathbf{I}_{n_x}, \mathbf{0}_{n_x \times (n_\gamma - n_x)}]$ .

**Remark 7.** In this work, a valid choice for the set  $\tilde{Z}$  required in Proposition 2 is obtained by taking the  $n_z - (n_x + n_w + n_v)$  bottom elements of the interval vector  $Z$ . This interval is computed using interval arithmetic as in Remark 3. Analogous choices are valid for  $\tilde{\Delta}$  and  $\tilde{\Gamma}$  in Remarks 5 and 6, respectively.

**Remark 8.** For implementation purposes, to avoid unnecessary computations, in case  $\mathbf{g}$  is linear in  $\mathbf{x}_k$  and  $\mathbf{v}_k$ , i.e.,  $\mathbf{g}(\mathbf{x}_k, \mathbf{v}_k) = \mathbf{C}\mathbf{x}_k + \mathbf{D}\mathbf{v}_k$ , with  $\mathbf{C} \in \mathbb{R}^{n_y \times n_x}, \mathbf{D} \in \mathbb{R}^{n_y \times n_v}$ , one can obtain  $\hat{X}_k$  as  $\hat{X}_k = \tilde{X}_k \cap_C (\mathbf{y}_k \oplus (-\mathbf{D}\mathbf{v}_k))$ , where  $\tilde{X}_k$  is the predicted set computed according to Remark 5.

**Remark 9.** An alternative to the prediction-update step described by (11) and Proposition 3 is to compute the prediction and update steps separately, as done in the previous literature (Alamo et al., 2005; Rego et al., 2021). This can be accomplished by using the enclosure obtained in Remark 5 and an adaptation of Remark 6 for  $k \geq 1$ , respectively. However, the computation of these steps separately would require to obtain the interval hull of a CZ enclosure twice per  $k$  instead of once. This results in an increase of computational cost since it requires the solution of linear programs.

All the set operations in (18) are computed by taking advantage of the properties of CZs and convex polytopes described in Section 2. If  $\tilde{Z}$  in Proposition 3 is obtained according to Remark 7, then it can be described as a zonotope with  $n_z - (n_x + n_w + n_v)$  generators. Let  $\hat{X}_{k-1}$  have  $n_{g_{k-1}}$  generators, and  $n_{c_{k-1}}$  constraints. Moreover, let  $P_\ell \cap P_y$  have  $n_{h_p}$  halfspaces and  $n_{c_p}$  equality constraints. With Cartesian products and linear image computed using (3) and (4), respectively, and using (8) for the intersection with  $P_\ell \cap P_y$ , the CZ enclosure  $\hat{X}_k$  obtained by (18) has  $n_{g_k} = n_{g_{k-1}} + n_{g_w} + n_{g_v} + n_z - (n_x + n_w + n_v) + n_{h_p}$  generators and  $n_{c_k} = n_{c_{k-1}} + n_{c_w} + n_{c_v} + n_{h_p} + n_{c_p}$  constraints.

It is noteworthy that  $n_z - (n_x + n_w + n_v), n_{h_p}$ , and  $n_{c_p}$  are constant values, which depend only on the (non-unique) factorizations of  $\mathbf{f}$  and  $\mathbf{g}$ . This implies that the complexity increase at each computation of (18) is linear, which is an important advantage with respect to the quadratic complexity growth in first-order Taylor expansion (Rego et al., 2021), and exponential complexity growth in pure convex polytope enclosures. However, both  $n_{h_p}$  and  $n_{c_p}$  are proportional to the number of factors  $n_z$ . Consequently, even with a linear growth, the enclosure  $\hat{X}_k$  can become intractable for more complicated functions due to the complexity of  $P_\ell \cap P_y$ . This can be mitigated by using well known complexity reduction methods of CZs (Scott et al., 2016), in addition to obtaining an equivalent polyhedral enclosure using less halfspaces and equality constraints, as shown in the next subsection.

#### 4.1. Equivalent enclosure with reduced set complexity

In this section, we demonstrate that some equality constraints in the polyhedron enclosure  $P_\ell \cap P_y$  obtained in Proposition 3 can be eliminated with no conservatism. This allows to compute a simpler set representation that is equivalent to (18). For  $j = \{1, \dots, n_z\}$ , let  $\alpha_j$  be defined as in Definition 2. For  $a, b < j$ , and constant scalars  $q_j \in \mathbb{R}$ , the operations related to such equality constraints are:

$$\begin{aligned} \alpha_j(z_a, z_b) &\triangleq z_a + z_b, & \alpha_j(z_a, z_b) &\triangleq z_a + q_j, \\ \alpha_j(z_a, z_b) &\triangleq z_a - z_b, & \alpha_j(z_a, z_b) &\triangleq q_j z_a. \end{aligned} \quad (19)$$

We denote  $\mathcal{I} \triangleq \{1, 2, \dots, n_z\}$ , and  $\mathcal{I}_e \subset \mathcal{I}$  is the set of indices  $j \in \mathcal{I}$  such that  $\alpha_j$  is given by one of the operations above.

Let  $\mathbf{z} \in P_\ell \cap P_y$ , and  $P_\ell \cap P_y \triangleq (\mathbf{H}_p, \mathbf{k}_p, \mathbf{A}_p, \mathbf{b}_p)_P$ . To proceed, we partition  $\mathbf{z}$  as  $(\mathbf{z}_e, \mathbf{z}_r) \in \mathbb{R}^{n_z}$ , where: (i)  $\mathbf{z}_e \in \mathbb{R}^{n_e}$  denote the elements to be eliminated, given by  $z_j = \alpha_j(\mathbf{z})$  for all  $j \in \mathcal{I}_e$  in ascending order, and (ii)  $\mathbf{z}_r \in \mathbb{R}^{n_r}$  denote the retained elements, given by  $z_j = \alpha_j(\mathbf{z})$  for all  $j \in \mathcal{I} \setminus \mathcal{I}_e$ , also in ascending

order. Accordingly, we also partition and reorder the equality constraints  $\mathbf{A}_p \mathbf{z} = \mathbf{b}_p$ , as

$$\begin{bmatrix} \mathbf{A}_{ee} & \mathbf{A}_{er} \\ \mathbf{A}_{re} & \mathbf{A}_{rr} \end{bmatrix} \begin{bmatrix} \mathbf{z}_e \\ \mathbf{z}_r \end{bmatrix} = \begin{bmatrix} \mathbf{b}_e \\ \mathbf{b}_r \end{bmatrix} \quad (20)$$

where the columns of  $\mathbf{A}_{ee} \in \mathbb{R}^{n_e \times n_e}$  are ordered according to  $j \in \mathcal{I}_e$ . Note that the rows of  $[\mathbf{A}_{ee} \ \mathbf{A}_{er}]$  are associated to the equality constraints obtained by the corresponding  $Q_j$ . The respective formulas in Section 3.1, which are exactly the operations in (19), in addition to the fact that  $a, b < j$ , ensure that  $\mathbf{A}_{ee}$  is a lower triangular matrix with ones on its diagonal. Therefore, this matrix is always invertible.

Accordingly, we also partition the inequality constraints  $\mathbf{H}_p \mathbf{z} \leq \mathbf{k}_p$  as  $\mathbf{H}_e \mathbf{z}_e + \mathbf{H}_r \mathbf{z}_r \leq \mathbf{k}_p$ , and define the convex polytope  $\hat{P} \triangleq (\hat{\mathbf{H}}, \hat{\mathbf{k}}, \hat{\mathbf{A}}, \hat{\mathbf{b}})_p$ , where

$$\begin{aligned} \hat{\mathbf{H}} &\triangleq (\mathbf{H}_r - \mathbf{H}_e \mathbf{A}_{ee}^{-1} \mathbf{A}_{er}), & \hat{\mathbf{k}} &\triangleq \mathbf{k} - \mathbf{H}_e \mathbf{A}_{ee}^{-1} \mathbf{b}_e, \\ \hat{\mathbf{A}} &\triangleq (\mathbf{A}_{rr} - \mathbf{A}_{re} \mathbf{A}_{ee}^{-1} \mathbf{A}_{er}), & \hat{\mathbf{b}} &\triangleq \mathbf{b}_r - \mathbf{A}_{re} \mathbf{A}_{ee}^{-1} \mathbf{b}_e. \end{aligned} \quad (21)$$

**Lemma 1.** Let  $\mathbf{z}, \mathbf{z}_e, \mathbf{z}_r, P_\ell \cap P_y = (\mathbf{H}_p, \mathbf{k}_p, \mathbf{A}_p, \mathbf{b}_p)_p$  and  $\hat{P} = (\hat{\mathbf{H}}, \hat{\mathbf{k}}, \hat{\mathbf{A}}, \hat{\mathbf{b}})_p$  as defined above. Then,  $\mathbf{z} \in P_\ell \cap P_y \iff \mathbf{z}_r \in \hat{P}$ .

*Proof.* Consider any  $\mathbf{z} \in P_\ell \cap P_y$ . Then, by the definition of  $\mathbf{z}_e$  and  $\mathbf{z}_r$ , both (20) and  $\mathbf{H}_e \mathbf{z}_e + \mathbf{H}_r \mathbf{z}_r \leq \mathbf{k}_p$  hold. Then, partially solving (20) in  $\mathbf{z}_e$  gives

$$\mathbf{z}_e = \mathbf{A}_{ee}^{-1} (\mathbf{b}_e - \mathbf{A}_{er} \mathbf{z}_r). \quad (22)$$

Replacing (22) into the bottom part of (20), leads to

$$(\mathbf{A}_{rr} - \mathbf{A}_{re} \mathbf{A}_{ee}^{-1} \mathbf{A}_{er}) \mathbf{z}_r = \mathbf{b}_r - \mathbf{A}_{re} \mathbf{A}_{ee}^{-1} \mathbf{b}_e. \quad (23)$$

Additionally, replacing (22) in  $\mathbf{H}_e \mathbf{z}_e + \mathbf{H}_r \mathbf{z}_r \leq \mathbf{k}_p$  leads to

$$(\mathbf{H}_r - \mathbf{H}_e \mathbf{A}_{ee}^{-1} \mathbf{A}_{er}) \mathbf{z}_r \leq \mathbf{k}_p - \mathbf{H}_e \mathbf{A}_{ee}^{-1} \mathbf{b}_e. \quad (24)$$

Since  $\mathbf{z}_r$  satisfies both (23) and (24), then by (21),  $\mathbf{z}_r \in \hat{P}$ .

Conversely, consider any  $\mathbf{z}_r \in \hat{P}$ . Then, by definition, both (23) and (24) hold. By the definition of  $\mathbf{z}_e$ , we have that  $\mathbf{A}_{ee} \mathbf{z}_e + \mathbf{A}_{er} \mathbf{z}_r = \mathbf{b}_e$ . Then, it is true that  $\mathbf{A}_{er} \mathbf{z}_r = \mathbf{b}_e - \mathbf{A}_{ee} \mathbf{z}_e$ . Replacing this result in (23) and (24) gives  $\mathbf{A}_{re} \mathbf{z}_e + \mathbf{A}_{rr} \mathbf{z}_r = \mathbf{b}_r$  and  $\mathbf{H}_e \mathbf{z}_e + \mathbf{H}_r \mathbf{z}_r \leq \mathbf{k}_p$ , respectively. By reordering these equalities and inequalities according to  $j \in \{1, \dots, n_z\}$  in ascending order, we have that  $\mathbf{A}_p \mathbf{z} = \mathbf{b}_p$  and  $\mathbf{H}_p \mathbf{z} \leq \mathbf{k}_p$ , which implies  $\mathbf{z} \in P_\ell \cap P_y$ . ■

To develop an alternate expression for (18) in terms of  $\mathbf{z}_r$ , it is necessary to replace the set  $\tilde{Z} \ni \tilde{\zeta}(\mathbf{s}, \mathbf{u}_{k-1})$  by an appropriate enclosure such that no information on  $\mathbf{z}_e$  is lost. Let  $\zeta_r$  denote the factors associated to  $\mathbf{z}_r$ , respectively. Define  $\hat{Z}$  in such a way that  $\mathbf{z}_r = \zeta_r(\mathbf{s}, \mathbf{u}_{k-1}) \in S \times \hat{Z}$  for all  $\mathbf{s} \in S$ . The set  $\hat{Z}$  must be chosen such that  $\mathbf{z}_r \in S \times \hat{Z} \implies \mathbf{z} \in S \times \tilde{Z}$ . If the latter holds, the alternate enclosure to (18) will be equivalent.

Additionally, by the operations in (19), we note that the eliminated elements  $\mathbf{z}_e$  can be described as a composite function of at least one  $\alpha_j$  with  $\mathbf{z}_r$  as input. We denote this mapping as  $\mathbf{z}_e = \tilde{\alpha}(\mathbf{z}_r)$ . To proceed, the assumption below is required.

**Assumption 1.** The interval vector  $Z$  and the set  $\tilde{Z}$  required in Propositions 2 and 3 are computed using interval arithmetic, following Remarks 3 and 7, respectively.

In the following, we show that if  $\hat{Z}$  is an interval obtained from the interval vector  $\tilde{Z}$  by removing the elements corresponding to  $j \in \mathcal{I}_e$ , then  $\mathbf{z}_r \in S \times \hat{Z} \implies \mathbf{z} \in S \times \tilde{Z}$ . For this to hold, it is enough to prove that  $\mathbf{z}_r \in S \times \hat{Z} \implies \mathbf{z}_e \in Z_e$ , where  $Z_e$  is an interval vector obtained by choosing the rows of  $\tilde{Z}$  associated to  $j \in \mathcal{I}_e$ .

**Lemma 2.** Let the interval vector  $Z$  be obtained following Assumption 1 for the composite function  $\ell$ . Consider the partitioning of  $Z$  into  $Z_e$  and  $Z_r$  according to the eliminated and retained elements, such that  $(\mathbf{z}_e, \mathbf{z}_r) \in Z_e \times Z_r$ . Then, for every  $\mathbf{z}_r$  in  $Z_r$ ,  $\mathbf{z}_e$  given by (22) lies in  $Z_e$ .

*Proof.* Since  $Z$  is obtained using interval arithmetic, following Remark 3, the operations performed to obtain  $Z_e$  are equivalent to the composite mapping  $\mathbf{z}_e = \tilde{\alpha}(\mathbf{z}_r)$  in real arithmetic. Then, it is true that  $\tilde{\alpha}(\mathbf{z}_r) \in Z_e$  for any  $\mathbf{z}_r \in Z_r$ . Additionally, by the definition of  $\mathbf{z}_e$  and  $\mathbf{z}_r$ , (22) holds. Since the latter is obtained by construction from  $\alpha_j$  given as in (19), and the same is true for the composite mapping  $\mathbf{z}_e = \tilde{\alpha}(\mathbf{z}_r)$ , then (22) and  $\mathbf{z}_e = \tilde{\alpha}(\mathbf{z}_r)$  are also equivalent in real arithmetic. Consequently, for any  $\mathbf{z}_r \in Z_r$ ,  $\mathbf{z}_e$  given by (22) also lies in  $Z_e$ . ■

Finally, to obtain an alternate expression for (18) we also partition  $\mathbf{f}(\mathbf{s}, \mathbf{u}_{k-1}) = \mathbf{E}_f \mathbf{z}$  as  $\mathbf{E}_f \mathbf{z} = \mathbf{E}_e \mathbf{z}_e + \mathbf{E}_r \mathbf{z}_r$ . Replacing (22) in this equation yields

$$\mathbf{f}(\mathbf{s}, \mathbf{u}_{k-1}) = (\mathbf{E}_r - \mathbf{E}_e \mathbf{A}_{ee}^{-1} \mathbf{A}_{er}) \mathbf{z}_r + (\mathbf{E}_e \mathbf{A}_{ee}^{-1} \mathbf{b}_e). \quad (25)$$

Therefore, the prediction-update step (18), with partially solved equality constraints in the polyhedral enclosure, is rewritten as

$$\hat{X}_k \triangleq \mathbf{G}_f((\hat{X}_{k-1} \times W \times V \times \hat{Z}) \cap \hat{P}) \oplus \mathbf{c}_f, \quad (26)$$

where  $\hat{Z}$  denotes the interval obtained from  $\tilde{Z}$  by removing the elements corresponding to  $j \in \mathcal{I}_e$ , and

$$\mathbf{G}_f \triangleq (\mathbf{E}_r - \mathbf{E}_e \mathbf{A}_{ee}^{-1} \mathbf{A}_{er}), \quad \mathbf{c}_f \triangleq (\mathbf{E}_e \mathbf{A}_{ee}^{-1} \mathbf{b}_e). \quad (27)$$

Note that, unlike (18), the new enclosure in (26) is not a projection of a constrained zonotope in the lifted space onto  $\mathbf{f}$ . It is now a linear transformation of a constrained zonotope by  $\mathbf{G}_f$ , with center displaced by  $\mathbf{c}_f$ .

**Proposition 4.** The CZ enclosures (18) and (26) are equivalent.

*Proof.* By Lemma 1,  $\mathbf{z} \in P_\ell \cap P_y \iff \mathbf{z}_r \in \hat{P}$ . Moreover, since  $\mathbf{z}_r$  is part of the vector  $\mathbf{z}$ , and  $\hat{Z}$  is part of the interval vector  $\tilde{Z}$ , then  $\mathbf{z} \in \hat{X}_{k-1} \times W \times V \times \hat{Z} \implies \mathbf{z}_r \in \hat{X}_{k-1} \times W \times V \times \hat{Z}$ . Since  $\hat{X}_{k-1} \times W \times V \times \hat{Z} \subseteq Z_r$ , Lemma 2 ensures that  $\mathbf{z}_r \in \hat{X}_{k-1} \times W \times V \times \hat{Z} \implies \mathbf{z} \in \hat{X}_{k-1} \times W \times V \times \tilde{Z}$ . Finally,  $\mathbf{G}_f \mathbf{z}_r + \mathbf{c}_f = \mathbf{E}_f \mathbf{z}$  holds for all  $(\mathbf{z}_e, \mathbf{z}_r) = \tilde{\mathbf{z}} \in \tilde{Z}$ , where  $\tilde{\mathbf{z}}$  and  $\tilde{Z}$  denote  $\mathbf{z}$  and  $Z$  with reordered components, respectively. Then, the proof is concluded. ■

Let  $\hat{X}_{k-1}$  have  $n_{g_{k-1}}$  generators and  $n_{c_{k-1}}$  constraints, and let  $P_\ell \cap P_y$  in Proposition 3 have  $n_{h_p}$  halfspaces and  $n_{c_p}$  equality



constraints. Let  $n_e$  be the number of elements eliminated using (22). Then, the CZ enclosure  $\hat{X}_k$  obtained by (26) has  $n_{g_k} = n_{g_{k-1}} + n_{g_w} + n_{g_v} + n_z - (n_x + n_w + n_v + n_e) + n_{h_p}$  generators and  $n_{c_k} = n_{c_{k-1}} + n_{c_w} + n_{c_v} + n_{h_p} + n_{c_p} - n_e$  constraints. In other words,  $\hat{X}_k$  obtained by (26) is an equivalent enclosure to (18) with  $n_e$  fewer generators and constraints. Thanks to this fact, the enclosure (26) is used in this paper.

#### 4.2. Proposed algorithm and implementation details

The full proposed method for set-based state estimation of nonlinear discrete-time systems with time horizon  $k \in [0, N]$  is given in Algorithm 1. The complexity reduction methods for CZs proposed in Scott et al. (2016), denoted as  $\text{red}(\cdot)$ , are applied to  $\hat{X}_k$  at the end of each time step  $k$ . This approach is usual in zonotope and CZ methods (Alamo et al., 2005; Rego et al., 2021), and necessary due to the complexity increase observed in (26), which, although linear in time, may result in intractable enclosures for large  $N$ .

In our implementation, Steps 7, 8 and 9 in Algorithm 1 are performed automatically thanks to object oriented programming and the extensive use of operator overloading. The input interval  $\square S$  is assigned to a user-defined class object, for which all operations described in Sections 3.1 and 3.2 are implemented. Then, by evaluating the nonlinear function  $\ell$  with the  $\square S$  object as input, each interval  $Z_j$  (Remark 3) and half-space enclosure  $Q_j$  is computed and stored in memory, giving  $Z$  and  $P_\ell$  at the end of the nonlinear function evaluation. This makes the process of obtaining the polyhedral relaxation straightforward, without requiring specific implementations for each nonlinear function to be investigated.

---

#### Algorithm 1 CZPR for state estimation of (9).

---

- 1: Let  $(X_0, W, V) \subset \mathbb{R}^{n_x} \times \mathbb{R}^{n_w} \times \mathbb{R}^{n_v}$  be constrained zonotopes, and  $(\mathbf{u}_k, \mathbf{y}_k) \in \mathbb{R}^{n_u} \times \mathbb{R}^{n_y}$ ,  $k \in [0, N]$ . These variables must satisfy  $(\mathbf{x}_0, \mathbf{w}_k, \mathbf{v}_k) \in X_0 \times W \times V$  and (9b);
  - 2: Obtain a factorable representation of the function  $\mathbf{g}(\mathbf{x}_k, \mathbf{v}_k)$ ;
  - 3: Compute  $\hat{X}_0$  according to Remark 6;
  - 4: Obtain a factorable representation of the composite function  $\ell(\mathbf{x}_{k-1}, \mathbf{w}_{k-1}, \mathbf{v}_k, \mathbf{u}_{k-1}) = \mathbf{g}(\mathbf{f}(\mathbf{x}_{k-1}, \mathbf{w}_{k-1}, \mathbf{u}_{k-1}), \mathbf{v}_k)$ ;
  - 5: **for**  $k = 1, \dots, N$  **do**
  - 6:    $S \leftarrow \hat{X}_{k-1} \times W \times V$ ;
  - 7:   Compute  $Z$  as in Remark 3 with  $\square S$  as input;
  - 8:   Compute  $Q_j$  for each  $\alpha_j$ ,  $j > n_x + n_w + n_v$ , using  $Z$ ;
  - 9:    $P_\ell \leftarrow \bigcap_{j=n_x+n_w+n_v+1}^{n_z} Q_j$  using (7);
  - 10:    $P_y \leftarrow (\_, \_, \mathbf{E}_\ell, \mathbf{y}_k)_P$ ;
  - 11:   Compute  $P_\ell \cap P_y$  using (7);
  - 12:   Obtain  $\hat{P} = (\hat{\mathbf{H}}, \hat{\mathbf{k}}, \hat{\mathbf{A}}, \hat{\mathbf{b}})_P$ ,  $\mathbf{G}_f$  and  $\mathbf{c}_f$  using (21) and (27);
  - 13:   Obtain  $\hat{Z}$  from  $Z$ ;
  - 14:    $\hat{X}_k \leftarrow \mathbf{G}_f((\hat{X}_{k-1} \times W \times V \times \hat{Z}) \cap \hat{P}) \oplus \mathbf{c}_f$ ;
  - 15:    $\hat{X}_k \leftarrow \text{red}(\hat{X}_k)$ ;
  - 16: **end for**
- 

## 5. Numerical examples

This section illustrates, through numerical simulations, the advantages of the proposed CZ state estimation method based

on polyhedral relaxations (Algorithm 1), and compares with results obtained using: (i) the CZ-based mean value extension (CZMV) described in Rego et al. (2021), with heuristic  $C2$  therein for the approximation point; and (ii) the CZ enclosures obtained using DC programming described in de Paula et al. (2024), denoted as CZDC, using Proposition 4 therein for DC function decomposition, in addition to using the interval hull of the respective CZ enclosures for vertex evaluations. Numerical simulations were performed using MATLAB 9.1 and Gurobi 10.0.1 for solving LPs. For all methods, the number of constraints and generators in the CZs is limited by using the reduction methods in Scott et al. (2016). For comparison, we compute the  $n_x$ -th root of the operators  $\text{Vol}_\square(\hat{X}_k)$  and  $\text{Vol}_\diamond(\hat{X}_k)$ , which are defined as the exact volumes of  $\square\hat{X}_k$  and  $\diamond\hat{X}_k$ , respectively. The latter notation stands for a tight parallelotope enclosure of  $\hat{X}_k$  obtained by applying Proposition 3 from de Paula et al. (2024) to  $\hat{X}_k$ , using the parallelotope computed from reducing  $\hat{X}_k$  through constraint elimination and generator reduction as initial bound. Two different approximation metrics are used because the computation of the exact volumes of the CZ enclosures is intractable in general. We also define the geometric average  $n_x$ -th root volume ratios  $\text{GAVR}_\square$  and  $\text{GAVR}_\diamond$ , i.e., the ratio of  $\sqrt[n_x]{\text{Vol}_\square(\hat{X}_k)}$  and  $\sqrt[n_x]{\text{Vol}_\diamond(\hat{X}_k)}$ , respectively, provided by one method over the same metric provided by another method at  $k$ , geometrically averaged over all time steps.

### 5.1. Example 1

We first consider a discrete-time system with nonlinear dynamics and nonlinear measurement equations described by (Rego et al., 2021)

$$\begin{aligned} x_{1,k} &= 3x_{1,k-1} - \frac{x_{1,k-1}^2}{7} - \frac{4x_{1,k-1}x_{2,k-1}}{4 + x_{1,k-1}} + w_{1,k-1}, \\ x_{2,k} &= -2x_{2,k-1} + \frac{3x_{1,k-1}x_{2,k-1}}{4 + x_{1,k-1}} + w_{2,k-1}, \\ y_{1,k} &= x_{1,k} - \sin\left(\frac{x_{2,k}}{2}\right) + v_{1,k}, \\ y_{2,k} &= -x_{1,k}x_{2,k} + x_{2,k} + v_{2,k}. \end{aligned}$$

The uncertainties are bounded by  $\|\mathbf{w}_k\|_\infty \leq 0.8$  and  $\|\mathbf{v}_k\|_\infty \leq 0.4$ . The initial state is  $\mathbf{x}_0 = (5.2, 0.65)$  for simulation. The initial enclosure  $X_0$  is

$$X_0 = \left( \left[ \begin{array}{ccc} 0.5 & 1 & -0.5 \\ 0.5 & 0.5 & 0 \end{array} \right], \left[ \begin{array}{c} 5 \\ 0.5 \end{array} \right] \right)_Z. \quad (28)$$

The numbers of generators and constraints are limited to 20 and 8, respectively.

Figures 2 and 3 show  $\sqrt[n_x]{\text{Vol}_\square(\hat{X}_k)}$  and  $\sqrt[n_x]{\text{Vol}_\diamond(\hat{X}_k)}$ , respectively, for the enclosures  $\hat{X}_k$  obtained using CZMV, CZDC, and CZPR, for  $k \in [0, 100]$ . The enclosures provided by CZDC diverge quickly, while those produced by both CZMV and CZPR remain bounded. However, CZPR provides notably tighter enclosures than CZMV, with 49.79% and 53.38% CZPR-to-CZMV  $\text{GAVR}_\square$  and  $\text{GAVR}_\diamond$ , respectively. In addition, the average computational times per time step of CZMV and CZPR were 34.4 ms and 68.6 ms, respectively. The computational

times of CZPR were higher than CZMV for this example because the lifted polyhedral relaxation of the composite function  $\ell$  leads to a more complex enclosure than the one obtained by CZMV, requiring more computational effort by the order reduction methods. Figure 4 compares the sets  $\hat{X}_{40}$  provided by CZMV and CZPR, illustrating the difference in conservatism between the two methods for this example.

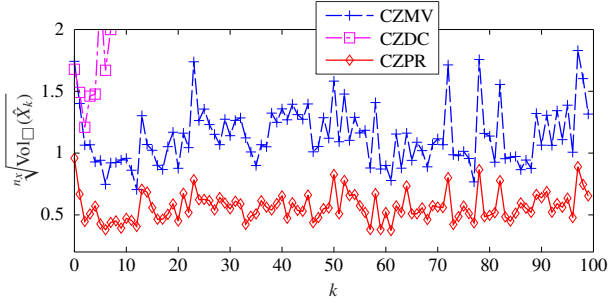


Figure 2: The  $n_x$ -th root of the volume of  $\square\hat{X}_k$  obtained using CZMV (+), CZDC ( $\square$ ), and CZPR ( $\diamond$ ), for Example 1.

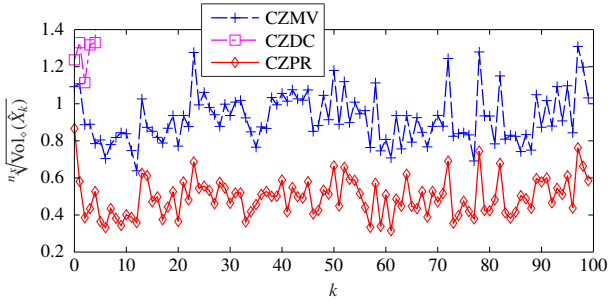


Figure 3: The  $n_x$ -th root of the volume of  $\diamond\hat{X}_k$  obtained using CZMV (+), CZDC ( $\square$ ), and CZPR ( $\diamond$ ), for Example 1.

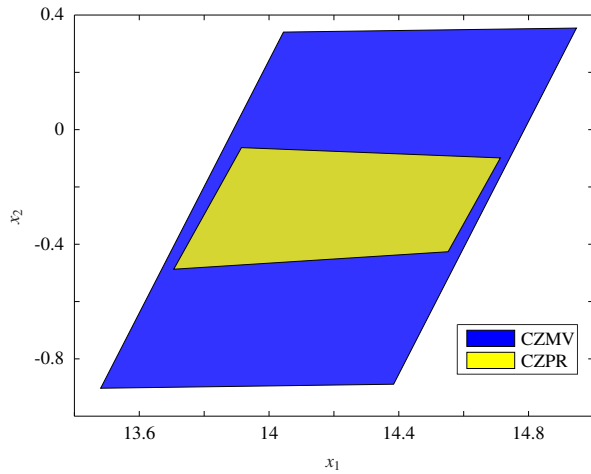


Figure 4: The enclosures  $\hat{X}_k$  for  $k = 40$  for Example 1, obtained using CZMV (blue) and CZPR (yellow).

## 5.2. Example 2

Consider a continuous-stirred tank reactor described by a discrete-time system with nonlinear dynamics given by (Yang & Scott, 2020)

$$\begin{aligned} x_{1,k} &= x_{1,k-1} + T_s[-w_{3,k-1}x_{1,k-1}x_{2,k-1} - \kappa_2x_{1,k-1}x_{3,k-1} \\ &\quad + \kappa_1(w_{1,k-1} - 2x_{1,k-1})], \\ x_{2,k} &= x_{2,k-1} + T_s[-w_{3,k-1}x_{1,k-1}x_{2,k-1} + \kappa_1(w_{2,k-1} - 2x_{2,k-1})], \\ x_{3,k} &= x_{3,k-1} + T_s[w_{3,k-1}x_{1,k-1}x_{2,k-1} - \kappa_2x_{1,k-1}x_{3,k-1} - 2\kappa_1x_{3,k-1}], \\ x_{4,k} &= x_{4,k-1} + T_s[\kappa_2x_{1,k-1}x_{3,k-1} - 2\kappa_1x_{4,k-1}], \end{aligned} \quad (29)$$

and linear measurement equations described by

$$\begin{aligned} y_{1,k} &= x_{1,k} + x_{2,k} + x_{3,k} + v_{1,k}, \\ y_{2,k} &= x_{2,k} + x_{3,k} + x_{4,k} + v_{2,k}, \\ y_{3,k} &= x_{1,k} + x_{4,k} + v_{3,k}, \end{aligned} \quad (30)$$

The parameters are  $\kappa_1 = 0.05 \text{ min}^{-1}$ ,  $\kappa_2 = 0.4 \text{ M}^{-1}\text{min}^{-1}$ , and  $T_s = 0.015 \text{ min}$ , while uncertainties are bounded by  $w_{1,k} \in [0.9, 1.1] \text{ M}$ ,  $w_{2,k} \in [0.8, 1.0] \text{ M}$ ,  $w_{3,k} \in [10, 50] \text{ M}$ ,  $|v_{1,k}| \leq 0.01$ ,  $|v_{2,k}| \leq 0.01$ , and  $|v_{3,k}| \leq 0.001$ . For simulation purposes, the initial state is  $\mathbf{x}_0 = (0.036, 0.038, 0.36, 0.052)$ , whereas  $X_0 = (0.01 \cdot \mathbf{I}_4, (0.036, 0.038, 0.36, 0.052))_{\mathcal{Z}}$ . The numbers of generators and constraints are limited to 60 and 20, respectively.

Figures 5 and 6 show  $\sqrt[n_x]{\text{Vol}_\square(\hat{X}_k)}$  and  $\sqrt[n_x]{\text{Vol}_\diamond(\hat{X}_k)}$ , respectively, for the enclosures  $\hat{X}_k$  obtained using CZMV, CZDC, and CZPR, for  $k \in [0, 600]$ . As in the previous example, the enclosures provided by CZDC diverge quickly, while both CZMV and CZPR remain bounded. However, once again, CZPR provides notably tighter enclosures than CZMV, with 12.90% and 23.65% CZPR-to-CZMV  $\text{GAVR}_\square$  and  $\text{GAVR}_\diamond$ , respectively. In addition, the average computational times per time step of CZMV and CZPR were 187.2 ms, 50.0 ms, respectively. In this example, the computational times of CZPR were considerably smaller than CZMV. This happens thanks to the fact that, despite the higher number of states in comparison to the previous example, the factorable representation of the system dynamics is very simple. Figure 7 compares the projections of the sets  $\hat{X}_{200}$  provided by CZMV and CZPR onto  $(x_1, x_2)$ , illustrating the significant difference in the conservatism of the two methods for this second example.

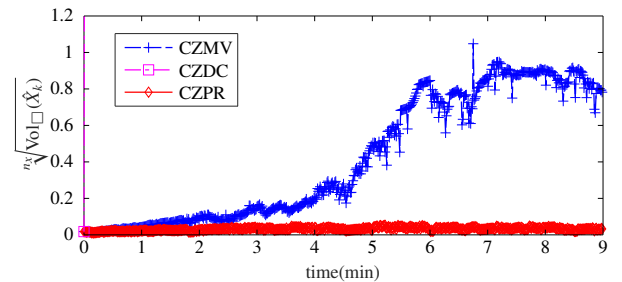


Figure 5: The  $n_x$ -th root of the volume of  $\square\hat{X}_k$  obtained using CZMV (+), CZDC ( $\square$ ), and CZPR ( $\diamond$ ), for Example 2

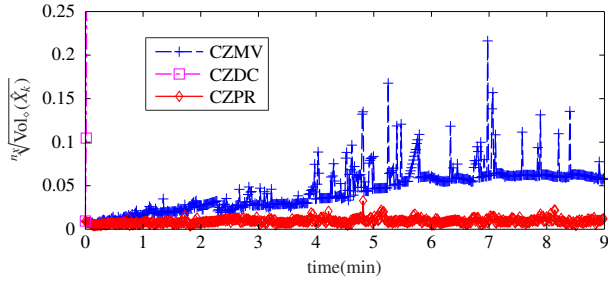


Figure 6: The  $n_x$ -th root of the volume of  $\hat{X}_k$  obtained using CZMV (+), CZDC (x), and CZPR (o), for Example 2.

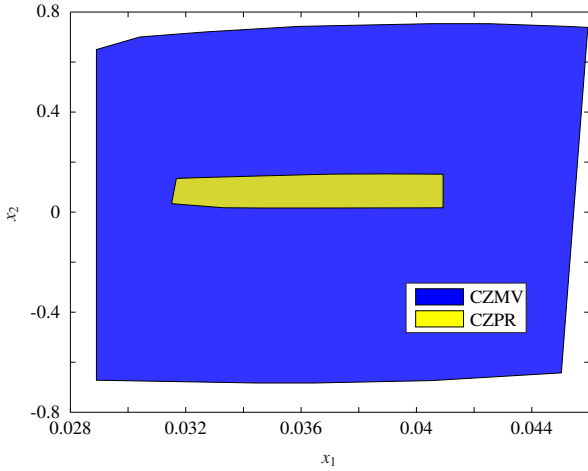


Figure 7: The projection of the enclosures  $\hat{X}_k$  into  $(x_1, x_2)$ , for  $k = 200$  for Example 2, obtained using CZMV (blue) and CZPR (yellow), respectively.

### 5.3. Example 3

Consider a planar robotic arm with two revolute joints as shown in Figure 8, where points  $p_1$  and  $p_2$  are located at the revolute joints and  $p_3$  is located at the end effector, whereas points  $q_1$  and  $q_2$  correspond to the centers of mass of each link. Through Euler discretization, the dynamics of this system are described by the nonlinear equations (D'Amato et al., 2011):

$$\mathbf{x}_k = \mathbf{x}_{k-1} + T_s \begin{bmatrix} x_{3,k-1} \\ x_{4,k-1} \\ \mathbf{M}(\mathbf{x}_{k-1})^{-1}(-\boldsymbol{\gamma}(\mathbf{x}_{k-1}) + \mathbf{q}(u_{k-1})) \end{bmatrix},$$

where  $\mathbf{q}(u) \triangleq (u, 0)$ ,  $\boldsymbol{\gamma}(\mathbf{x}) \triangleq (\gamma_1(\mathbf{x}), \gamma_2(\mathbf{x}))$ ,  $\gamma_1(\mathbf{x}) \triangleq \frac{1}{2}m_2l_1l_2 \sin(x_1 - x_2)x_4^2 + (k_1 + k_2)x_1 - k_2x_2 + (c_1 + c_2)x_3 - c_2x_4$ ,  $\gamma_2(\mathbf{x}) \triangleq -\frac{1}{2}m_2l_1l_2 \sin(x_1 - x_2)x_3^2 - k_2x_1 + k_2x_2 - c_2x_3 + c_2x_4$ ,

$$\mathbf{M}(\mathbf{x}) \triangleq \begin{bmatrix} \frac{1}{3}m_1l_1^2 + m_2l_1^2 & \frac{1}{2}m_2l_1l_2 \cos(x_1 - x_2) \\ \frac{1}{2}m_2l_1l_2 \cos(x_1 - x_2) & \frac{1}{3}m_2l_2^2 \end{bmatrix}.$$

Above,  $l_1 = 3$  m,  $l_2 = 2$  m,  $m_1 = 2$  kg and  $m_2 = 1$  kg, denote the lengths and masses of the links, respectively, whereas  $c_1 = 10$  N·m/(rad/s) and  $c_2 = 1$  N·m/(rad/s) are friction coefficients, and  $k_1 = 7$  N·m/rad and  $k_2 = 5$  N·m/rad are stiffness coefficients. The system input  $u_k \in \mathbb{R}$  is the torque applied to the first revolute joint. Moreover,  $x_1 \triangleq \theta_1$  and  $x_2 \triangleq \theta_2$  are the angles of

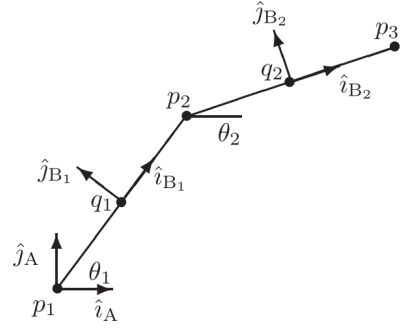


Figure 8: Planar robotic arm.

the links with respect to the inertial frame, whereas  $x_3 \triangleq \dot{\theta}_1$  and  $x_4 \triangleq \dot{\theta}_2$ . We consider a challenging scenario in which only the position of the end effector is measured, i.e.,

$$\mathbf{y}_k = \begin{bmatrix} \cos(x_{1,k})l_1 + \cos(x_{2,k})l_2 \\ \sin(x_{1,k})l_1 + \sin(x_{2,k})l_2 \end{bmatrix} + \mathbf{v}_k,$$

with  $\mathbf{v}_k \in \mathbb{R}^2$ ,  $\|\mathbf{v}_k\|_\infty \leq 0.01$ . The initial state is  $\mathbf{x}_0 = \mathbf{0}_{4 \times 1}$ , and

$$\mathbf{X}_0 = \left( \begin{bmatrix} 0.1745 & 0 & 0 & 0 \\ 0 & 0.1745 & 0 & 0 \\ 0 & 0 & 0.0873 & 0 \\ 0 & 0 & 0 & 0.0873 \end{bmatrix}, \mathbf{0}_{4 \times 1} \right)_Z.$$

The numbers of generators and constraints are limited to 60 and 20, respectively. The known input is  $u_k = 20 \sin(kt_s)$  N·m.

Figures 9 and 10 show  $\sqrt[n_x]{\text{Vol}_\square(\hat{X}_k)}$  and  $\sqrt[n_x]{\text{Vol}_\circ(\hat{X}_k)}$ , respectively, for the enclosures  $\hat{X}_k$  obtained using CZMV, CZDC, and CZPR, for  $k \in [0, 450]$ . In this example, the enclosures provided by both CZDC and CZMV diverge quickly, while only CZPR remains bounded. The average computational time per time step was 1.614 s for CZPR, showing that the proposed methodology is computationally expensive for this example. Besides the factorable representation being more complex than the previous examples (resulting in a higher number of factors), having more trigonometric functions required a substantial number of halfspaces to build the lifted polyhedral relaxation. Still, CZPR was the only method able to provide good enclosures in this case. Since these functional forms are very common in industry and robotics systems, further improvements to computational efficiency will be investigated in future work.

## 6. Conclusions

This paper developed a novel method for set-based state estimation of nonlinear discrete-time systems with bounded uncertainties with reduced conservatism. Guaranteed enclosures of the trajectories of the system states were obtained by combining essential properties of constrained zonotopes and polyhedral relaxations of factorable representations of nonlinear functions, in addition to the refinement of the obtained enclosures using nonlinear measurement equations. The new approach, CZPR, builds polyhedral relaxations of each operation composing the

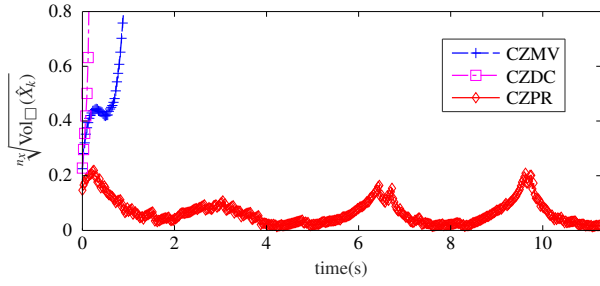


Figure 9: The  $n_x$ -th root of the volume of  $\square\hat{X}_k$  obtained using CZMV (+), CZDC ( $\square$ ), and CZPR ( $\diamond$ ), for Example 3.

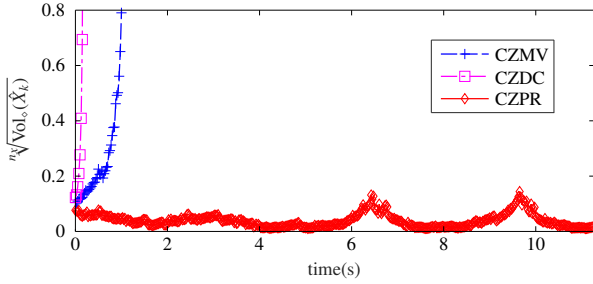


Figure 10: The  $n_x$ -th root of the volume of  $\diamond\hat{X}_k$  obtained using CZMV (+), CZDC ( $\square$ ), and CZPR ( $\diamond$ ), for Example 3.

nonlinear functions. While having linear complexity growth, this avoids both the linearization of the entire nonlinear mappings and the computation of linearization errors valid for the entire input set. Thanks to this fact, it was able to generate state enclosures that are less conservative than the ones obtained by other CZ methods from the literature based on the Mean Value Theorem and DC programming principles.

The advantages of CZPR were highlighted in three numerical examples. Nevertheless, as demonstrated in the third example, functional forms with high number of factors may result in enclosures with high number of generators and constraints, requiring substantial computational effort from order reduction methods. Future work will address the reduction of computational effort for state estimation of systems with such functional forms, for which CZPR was able to provide good enclosures, but with considerably high execution times.

## Appendix A. Polyhedral enclosure of the sine function

We first present the convex underestimator  $\beta_j^{\text{CV}}(z_a)$  for  $\beta_j(z_a) \triangleq \sin(z_a)$ ,  $z_a \in Z_a \triangleq [z_a^L, z_a^U]$ , based on the ideas described in Scott (2012). The latter develops an underestimator for  $Z_a \subset [\frac{3\pi}{2}, \frac{7\pi}{2}]$ , then extends it for the case of any input interval. Let

- $z_a^{S1}$  be the solution of  $\sin(z_a^U) - \sin(z_a) = (z_a^U - z_a) \cos(z_a)$  for  $z_a \in [\frac{3\pi}{2}, 2\pi]$ ,
- $z_a^{S2}$  be the solution of  $\sin(z_a) - \sin(z_a^L) = (z_a - z_a^L) \cos(z_a)$  for  $z_a \in [3\pi, \frac{7\pi}{2}]$ .

- If  $z_a^L \leq 2\pi$ ,  $z_a^{V1} \triangleq 2\pi$ . Otherwise,  $z_a^{V1} \triangleq z_a^{S1}$ .
- If  $z_a^U \leq 3\pi$ ,  $z_a^{V2} \triangleq 3\pi$ . Otherwise,  $z_a^{V2} \triangleq z_a^{S2}$ .
- $\rho^L \triangleq \text{med}(z_a^L, z_a^U, z_a^{V1})$ ,  $\rho^U \triangleq \text{med}(z_a^L, z_a^U, z_a^{V2})$ .

The operator  $\text{med}(\cdot)$  denotes the median of a collection of scalars. Additionally, define  $\eta : \mathbb{IR} \times \mathbb{R} \rightarrow \mathbb{R}$ , given by

$$\eta(Z_a, z_a) \triangleq \begin{cases} \sin(z_a) & \text{if } z_a \in [z_a^L, \rho^L] \\ \sin(\rho^L) + \frac{\sin(\rho^U) - \sin(\rho^L)}{\rho^U - \rho^L} (z_a - \rho^L) & \text{if } z_a \in (\rho^L, \rho^U] \\ \sin(z_a) & \text{if } z_a \in (\rho^U, z_a^U] \end{cases}$$

Note that  $\eta$  is a valid convex underestimator for  $Z_a \subset [\frac{3\pi}{2}, \frac{7\pi}{2}]$ . It is extended to a general input interval as follows. Define  $\varpi(z_a) \triangleq \frac{1}{2\pi}z_a + \frac{1}{4}$ , and let  $\varpi^L \triangleq \text{floor}(\varpi(z_a^L))$ , and  $\varpi^U \triangleq \varpi(z_a^U) - 1$  if  $\varpi(z_a^U)$  is an integer,  $\varpi^U \triangleq \text{floor}(\varpi(z_a^U))$  otherwise. Furthermore, define the functions  $\gamma(z_a) \triangleq z_a - 2(\varpi^L - 1)\pi$ ,  $\psi(z_a) \triangleq z_a - 2(\varpi^U - 1)\pi$ , and transformed intervals

- $\Gamma = [\gamma^L, \gamma^U] \triangleq [\gamma(z_a^L), \min(\gamma(z_a^U), \frac{7\pi}{2})]$ ,
- $\Psi = [\psi^L, \psi^U] \triangleq [\frac{3\pi}{2}, \psi(z_a^U)]$ .

Then, a valid convex underestimator  $\beta_j^{\text{CV}}(z_a)$  for any  $z_a \in Z_a \in \mathbb{IR}$  is given by

$$\beta_j^{\text{CV}}(z_a) \triangleq \begin{cases} \eta(\Gamma, \gamma(z_a)) & \text{if } \gamma(z_a) \leq \frac{7\pi}{2}, \\ \eta(\Psi, \psi(z_a)) & \text{if } \psi(z_a) \geq \frac{3\pi}{2}, \\ -1 & \text{otherwise.} \end{cases} \quad (\text{A.1})$$

We now describe a method to obtain the polyhedral relaxation  $Q_j^{\text{CV}}$ . By the definition of  $\beta_j^{\text{CV}}(z_a)$ , at most three regions must be investigated separately.

*Region 1.* All  $z_a \in Z_a$  such that  $\gamma(z_a) \leq \frac{7\pi}{2}$ . Note that this region exists only if at least one  $z_a \in Z_a$  satisfies this inequality. This is true if  $\gamma(z_a^L) \leq \frac{7\pi}{2}$ .

*Region 2.* All  $z_a \in Z_a$  such that  $\psi(z_a) \geq \frac{3\pi}{2}$ . Similarly to Region 1, the existence of this region is verified if  $\psi(z_a^U) \geq \frac{3\pi}{2}$ .

*Region 3.* All  $z_a \in Z_a$  such that  $\gamma(z_a) > \frac{7\pi}{2}$  or  $\psi(z_a) < \frac{3\pi}{2}$ . The existence of this region is verified if  $\gamma(z_a^U) > \frac{7\pi}{2}$  or  $\psi(z_a^L) < \frac{3\pi}{2}$ . The convex relaxation for this region is trivial and is given by the inequality  $z_a > -1$ .

If Region 1 exists, by the definition of the function  $\eta$ , at most three subregions within Region 1 must be analyzed separately. The investigation for Region 2 is analogous and therefore will be omitted.

*Subregion 1a.* All  $z_a \in Z_a$  such that  $\gamma(z_a) \in (\rho^L, \rho^U]$ . This subregion exists only if  $\rho^L < \rho^U$ . Note that both  $\rho^L$  and  $\rho^U$  are now evaluated in terms of  $\Gamma$  and  $\gamma(z_a)$ , since we are investigating  $\eta(\Gamma, \gamma(z_a))$ . The convex relaxation for this subregion is the inequality  $\gamma(z_a) \geq \sin(\rho^L) + \frac{\sin(\rho^U) - \sin(\rho^L)}{\rho^U - \rho^L} (\gamma(z_a) - \rho^L)$ .

*Subregion 1b.* All  $z_a \in Z_a$  such that  $\gamma(z_a) \in [\gamma^L, \rho^L]$ . This subregion must be analyzed only if  $\rho^L > \gamma^L$ . The halfspaces for this subregion are obtained by linearizing  $\sin(\gamma(z_a))$  at  $\gamma^L$ ,  $\gamma^{LM} \triangleq \text{mid}([\gamma^L, \rho^L])$ , and  $\rho^L$  leading to the inequalities  $\gamma(z_a) \geq \cos(\gamma^L)(\gamma(z_a) - \gamma^L) + \sin(\gamma^L)$ ,  $\gamma(z_a) \geq \cos(\gamma^{LM})(\gamma(z_a) - \gamma^{LM}) + \sin(\gamma^{LM})$ , and  $\gamma(z_a) \geq \cos(\rho^L)(\gamma(z_a) - \rho^L) + \sin(\rho^L)$ .

*Subregion 1c.* All  $z_a \in Z_a$  such that  $\gamma(z_a) \in (\rho^U, \gamma^U]$ . This subregion must be analyzed only if  $\gamma^U > \rho^U$ . The halfspaces for this subregion are obtained by linearizing  $\sin(\gamma(z_a))$  at  $\rho^U$ ,  $\gamma^{UM} \triangleq \text{mid}([\rho^U, \gamma^U])$ , and  $\gamma^U$  leading to the inequalities  $\gamma(z_a) \geq \cos(\rho^L)(\gamma(z_a) - \rho^L) + \sin(\rho^L)$ ,  $\gamma(z_a) \geq \cos(\gamma^{UM})(\gamma(z_a) - \gamma^{UM}) + \sin(\gamma^{UM})$ , and  $\gamma(z_a) \geq \cos(\gamma^U)(\gamma(z_a) - \gamma^U) + \sin(\gamma^U)$ .

These inequalities are written in terms of the input  $z_a$  by replacing  $\gamma(z_a)$  with its definition. The convex relaxation  $Q_j^{CV}$  is then obtained by collecting the inequalities from Subregions 1a, 1b and 1c, with the inequalities obtained by the analogous Subregions 2a, 2b, and 2c (replacing  $\psi(z_a)$  therein with its definition), in addition to Region 3. Note that the number of inequalities in  $Q_j^{CV}$  varies according to the existence conditions of the respective regions.

According to Scott (2012), a valid concave overestimator of  $\sin(z_a)$  for  $z_a \in Z_a$  is given by  $\beta_j^{CC}(z_a) \triangleq -\beta_j^{CV}(z_b)$  for  $z_b \in Z_b$ , where  $z_b \triangleq -z_a$  and  $Z_b \triangleq -Z_a$ . Then, the derivation of the concave relaxation  $Q_j^{CC}$  is analogous to  $Q_j^{CV}$  using a simple variable transformation. The polyhedron relaxation  $Q_j \supseteq \{z \in Z : z_j = \sin(z_a)\}$  is given by  $Q_j^{CV} \cap Q_j^{CC}$ .

## References

Alamo, T., Bravo, J., & Camacho, E. (2005). Guaranteed state estimation by zonotopes. *Automatica*, 41, 1035–1043.

Alamo, T., Bravo, J. M., Redondo, M. J., & Camacho, E. F. (2008). A set-membership state estimation algorithm based on DC programming. *Automatica*, 44, 216–224.

Althoff, M., Frehse, G., & Girard, A. (2021). Set Propagation Techniques for Reachability Analysis. *Annual Review of Control, Robotics, and Autonomous Systems*, 4, 369–395.

Combastel, C. (2005). A state bounding observer for uncertain non-linear continuous-time systems based on zonotopes. In *Proc. of the 44th IEEE Conference on Decision and Control, and 2005 European Control Conference* (pp. 7228–7234).

D’Amato, A. M., Ali, A., Springmann, J. C., Cutler, J. W., Ridley, A. J., & Bernstein, D. S. (2011). Adaptive state estimation for nonminimum-phase systems with uncertain harmonic inputs. In *Proc. of 2011 AIAA Guidance, Navigation and Control Conference* (pp. 1–18).

Jaulin, L. (2016). Inner and outer set-membership state estimation. *Reliable Computing*, 22, 47–55.

Kochdumper, N., & Althoff, M. (2023). Constrained polynomial zonotopes. *Acta Informatica*, 60, 279–316.

Kühn, W. (1998). Rigorously computed orbits of dynamical systems without the wrapping effect. *Computing*, 61, 47–67.

McCormick, G. P. (1976). Computability of global solutions to factorable non-convex programs: Part I — Convex underestimating problems. *Mathematical Programming*, 10, 147–175.

Moore, R. E., Kearfott, R. B., & Cloud, M. J. (2009). *Introduction to Interval Analysis*. Philadelphia, PA, USA: SIAM.

Mu, B., & Scott, J. K. (2024). Set-based fault diagnosis for uncertain nonlinear systems. *Computers & Chemical Engineering*, 180, 108479.

Pan, Z., & Liu, F. (2023). Nonlinear set-membership state estimation based on the Koopman operator. *International Journal of Robust and Nonlinear Control*, 33, 2703–2721.

de Paula, A. A., Raimondo, D. M., Raffo, G. V., & Teixeira, B. O. (2024). Set-based state estimation for discrete-time constrained nonlinear systems: An approach based on constrained zonotopes and DC programming. *Automatica*, 159, 111401.

Raghuraman, V., & Koeln, J. P. (2022). Set operations and order reductions for constrained zonotopes. *Automatica*, 139, 110204.

Rego, B. S., Locatelli, D., Raimondo, D. M., & Raffo, G. V. (2022). Joint state and parameter estimation based on constrained zonotopes. *Automatica*, 142, 110425.

Rego, B. S., Raffo, G. V., Terra, M. H., & Scott, J. K. (2024). Reachability analysis of nonlinear discrete-time systems using polyhedral relaxations and constrained zonotopes. In *Proc. of the 63rd IEEE Conference on Decision and Control* (pp. 7032–7037).

Rego, B. S., Raimondo, D. M., & Raffo, G. V. (2018). Set-based state estimation of nonlinear systems using constrained zonotopes and interval arithmetic. In *Proc. of the 2018 European Control Conference* (pp. 1584–1589).

Rego, B. S., Scott, J. K., Raimondo, D. M., & Raffo, G. V. (2021). Set-valued state estimation of nonlinear discrete-time systems with nonlinear invariants based on constrained zonotopes. *Automatica*, 129, 109628.

Scott, J. K. (2012). *Reachability Analysis and Deterministic Global Optimization of Differential-Algebraic Systems*. Ph.D. thesis Massachusetts Institute of Technology.

Scott, J. K., Raimondo, D. M., Marseglia, G. R., & Braatz, R. D. (2016). Constrained zonotopes: a new tool for set-based estimation and fault detection. *Automatica*, 69, 126–136.

Shamma, J. S., & Tu, K.-Y. (1997). Approximate set-valued observers for nonlinear systems. *IEEE Transactions on Automatic Control*, 42, 648–658.

Siefert, J. A., Bird, T. J., Thompson, A. F., Glunt, J. J., Koeln, J. P., Jain, N., & Pangborn, H. C. (2024). Reachability Analysis Using Hybrid Zonotopes and Functional Decomposition. ArXiv:2304.06827.

Silvestre, D. (2022). Constrained convex generators: A tool suitable for set-based estimation with range and bearing measurements. *IEEE Control Systems Letters*, 6, 1610–1615.

Simon, D. (2010). Kalman filtering with state constraints: a survey of linear and nonlinear algorithms. *IET Control Theory and Applications*, 4, 1303–1318.

Tawarmalani, M., & Sahinidis, N. V. (2002). *Convexification and Global Optimization in Continuous and Mixed-Integer Nonlinear Programming* volume 65 of *Nonconvex Optimization and Its Applications*. Boston, MA: Springer US.

Tawarmalani, M., & Sahinidis, N. V. (2005). A polyhedral branch-and-cut approach to global optimization. *Mathematical Programming*, 103, 225–249.

Tottoli, A., de Paula, A. A., Raffo, G. V., Teixeira, B. O., & Raimondo, D. M. (2023). Set-based state estimation of a Li-ion cell using DC programming and constrained zonotopes. In *Proc. of the 22nd IFAC World Congress* (pp. 7147–7153).

Wang, Z., Shen, X., Liu, H., Meng, F., & Zhu, Y. (2022). Dual Set Membership Filter With Minimizing Nonlinear Transformation of Ellipsoid. *IEEE Transactions on Automatic Control*, 67, 2405–2418.

Yang, X., & Scott, J. K. (2018a). Accurate Set-Based State Estimation for Nonlinear Discrete-Time Systems using Differential Inequalities with Model Redundancy. In *2018 IEEE Conference on Decision and Control (CDC)* (pp. 680–685). IEEE.

Yang, X., & Scott, J. K. (2018b). A comparison of zonotope order reduction techniques. *Automatica*, 95, 378–384.

Yang, X., & Scott, J. K. (2020). Accurate uncertainty propagation for discrete-time nonlinear systems using differential inequalities with model redundancy. *IEEE Transactions on Automatic Control*, 65, 5043–5057.